

AN ABSTRACT OF THE THESIS OF

Jack Carter Riley for the M. S. in Physics
(Name) (Degree) (Major)

Date Thesis presented May 10, 1950 _ _ _ _ _

Title THE EFFECT OF A MAGNETIC FIELD ON THE UPPER FREQUENCY LIMIT
OF A TRIODE OSCILLATOR

Abstract Approved _____ (Major Professor) _____

Experimental evidence is presented which indicates that the upper frequency limit of a conventional resonant-line triode oscillator can be extended by the use of a magnetic field coaxial to the tube structure. Calculations of electron transit time are made which indicate that the frequency improvement may be the result of a virtual cathode in the grid region produced by certain combinations of magnetic field and positive grid potential. This virtual cathode decreases the cathode-plate spacing and increases the cathode-plate potential gradient. Both of these effects tend to decrease the cathode-plate transit time which is usually considered to be the major factor limiting the maximum operating frequency of a triode oscillator.

THE EFFECT OF A MAGNETIC FIELD ON THE UPPER
FREQUENCY LIMIT OF A TRIODE OSCILLATOR

by

JACK CARTER RILEY

A THESIS

submitted to


OREGON STATE COLLEGE

in partial fulfillment of
the requirements for the
degree of

MASTER OF SCIENCE


June 1950

APPROVED:




Head of Department of Physics

In Charge of Major



Chairman of School Graduate Committee



Dean of Graduate School

Date thesis is presented May 10, 1950

Typed by Loraine W. Riley

ACKNOWLEDGMENT

I would like to express my appreciation to those people and organizations who have helped to make possible the work reported herein.

Without the equipment provided by the Air Corps Millimeter Wave project, much of the time which was available for experimentation and research would have been lost in the construction of apparatus.

I would like to thank my adviser Dr. E. A. Yunker, for his guidance and assistance throughout the investigation; Dr. W. E. Milne and Dr. I. M. Hostetter of the Mathematics Department for assistance with the equation of electron motion; Mr. J. W. Griffith for the construction of the tube which was used; and Mr. Armon McDowell and others of the Physics Department Machine shop who were responsible for the construction of the tuning lines which were used.

TABLE OF CONTENTS

Introduction	1
Apparatus	4
Experimental Investigation	15
Calculations	27
Conclusions	32
Literature Cited	40
Appendix I	41
Appendix II	53

TABLE OF FIGURES

1.	Tubes used	5
2.	Tuning lines	5
3.	Tube connection to tuning lines	7
4.	Tube position between magnet poles	7
5.	Frequency indication	10
6.	Line-end shorting capacitor	10
7.	Operating position	11
8.	Circuit diagram	11
9.	Tube characteristics equipment	13
10.	Electrolytic tank	14
11.	Oscillating combinations of magnetic flux density and line length	16
12.	Oscillating combinations of magnetic flux density and line length	17
13.	Oscillating combinations of magnetic flux density and line length	18
14.	Grid current versus magnetic flux density	19
15.	Plate current versus magnetic flux density	20
16.	Effect of oscillation on grid and plate currents	22
17.	Frequency and wavelength versus line setting	23
18.	Frequency contours	23
19.	Tube characteristics versus magnetic flux density	25
20.	Effect of line-end shorting capacitor	26
21.	Electron transit times, potential measured	29
22.	Electron transit times, potential assumed	31
23.	Regions favoring oscillation improvement	34

24.	Nomographic chart of cut-off voltage	50
25.	Grid and plate cut-off conditions	49
26.	Electron velocity	53
27.	Transit time	54
28.	Induced grid current	54
29.	Applied grid current	55
30.	Vector diagram	56

LIST OF TABLES

I	Independent variables	15
II	Parameters for calculated electron paths	28

THE EFFECT OF A MAGNETIC FIELD ON THE UPPER FREQUENCY LIMIT OF A TRIODE OSCILLATOR

INTRODUCTION

In the Fall of 1947 a student in the Physics Department at Oregon State College stated that during the war he had seen an experiment carried out in which an ordinary triode vacuum tube in a conventional circuit had been operated in a magnetic field, and that frequencies had been produced which were higher than those normally obtainable with such tubes and circuits.

At the time that this statement was made the Air Corps Millimeter Wave Research project at Oregon State College was conducting experiments on certain types of resonant-line oscillators using triode tubes in magnetic fields. The parameters for one of these tubes were adjusted for operation as a conventional resonant-line oscillator with a magnetic field applied co-axially to the tube structure. From the results of this preliminary experiment it appeared that an increase in the upper frequency limit was possible. As a result the more extensive experiment reported herein was undertaken.

The upper frequency limit of a triode oscillator is normally considered to have been reached when the transit time between the cathode and plate of the tube is equal to one-half of the period of the oscillation. This is an empirical criterion which may be in error in either

direction in the case of any particular tube. As the frequency is increased the first detrimental effect of transit time is a large increase in grid conductance which necessitates a supply of power to the grid circuit. This conductance is the result of a transit-time produced phase shift in the current induced in the grid by the electrons traveling from the cathode to the plate. The limiting value of transit time is reached when the plate current lags the plate voltage by such an angle that oscillation is impossible. In many tubes the inductances of the leads, in series with the tube capacitances, limit tube operation to frequencies lower than those producing a prohibitive transit angle. In order to make any significant improvement in frequency limit it is usually considered necessary to change either the tube potentials or the tube construction in such a manner as to decrease the cathode-to-plate transit time.

Diode magnetron action was considered as a possible explanation for the observed increase in the upper frequency limit of the tube. Magnetron oscillations at the frequencies observed are possible for magnetic fields in the range of values used. However, it can be shown that the magnetron frequency is directly proportional to the strength of the magnetic field and, since the frequencies observed were dependent primarily on the tuning of the oscillator circuit, it was concluded that something other

than magnetron oscillation was responsible.

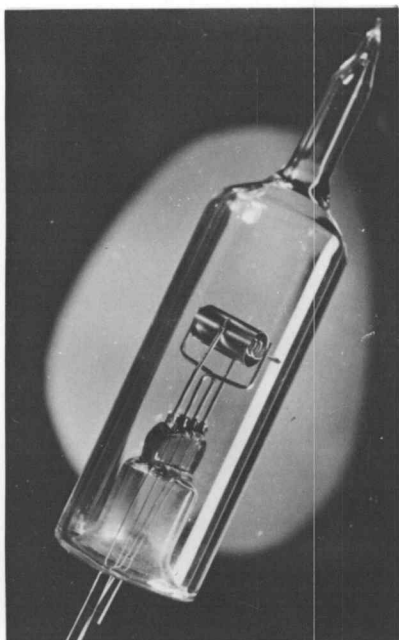
The increase in the maximum oscillation frequency, obtained by the addition of a magnetic field, appeared to be a new approach to the problem of obtaining high frequency oscillations. The experiments and calculations described in this thesis were made in an attempt to explain how this improvement in frequency limit is brought about and to find the extent to which it can be expected to affect the operation of a specific oscillator.

APPARATUS

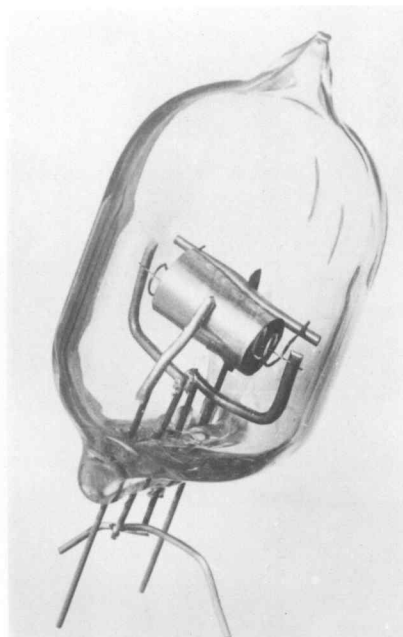
The facilities of the Air Corps Millimeter Wave Research project were made available for the investigation thus providing most of the necessary equipment. However, from the preliminary experiments it was concluded that a new tube should be designed and that improvements be made in the tuning lines.

The plate of the new tube was cylindrical in shape, 0.85 cm. in diameter, 1.5 cm. long, and was made of 5 mil tantalum. The grid consisted of an 11 turn helix 1.75 cm. long, and 0.45 cm. in diameter, made of 15 mil tungsten wire. An 8 mil tungsten wire, axial to the grid and plate, was used for the filament. Tungsten was used for the leads through the hard glass envelope. These leads were made as short in length and as large in diameter as possible in order to decrease the lead inductance and to improve the impedance match to the tuning lines. After preliminary evacuation the tube was outgassed by first baking all parts in a furnace, then heating the grid and plate to incandescence with a high-frequency induction heater. After two more hours of pumping it was sealed off at a pressure of approximately 10^{-6} mm of Hg. A photograph of the new tube, with the old one for comparison, is presented as Figure 1.

The resonant line oscillator is shown in the photograph, Figure 2 and in the schematic diagram, Figure 8. It



Old Tube



New Tube

Figure 1 TUBES USED

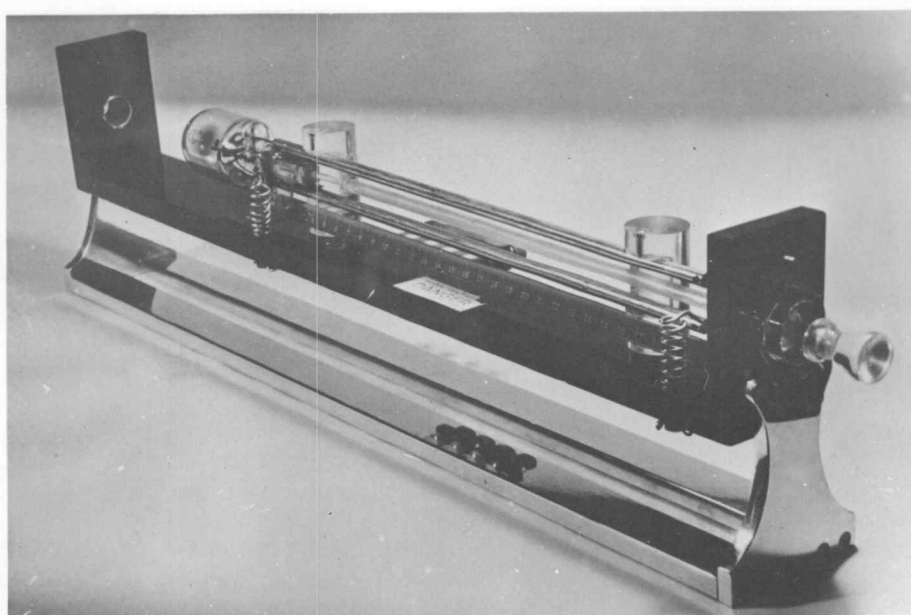


Figure 2 TUNING LINES

consisted of a pair of parallel rods or lines, 30 cm. long and 0.25 inches in diameter, one connected to the plate of the tube and the other to the grid. The tube connections can be seen in Figure 3 as can the capacitance shorting bar which served to adjust the electrical length of the lines. The oscillator was mounted so that the tube was located between the pole pieces of the electromagnet, with the filament parallel to the field, as shown in Figure 4.

The grid and plate potentials were obtained from conventional, regulated, direct current power supplies, which were capable of supplying 100 ma. of current at voltages continuously variable from 0 to 600 volts. Storage batteries provided current for both filament and magnetic field circuits. The voltages and currents for the plate and grid and the currents for the filament and magnetic field were indicated continuously on meters.

The magnetic flux density was measured by means of a flux meter consisting of a coil rotated at constant speed in the magnetic field. The voltage produced by the coil was indicated on a meter calibrated directly in flux density. The flux meter can be seen in Figure 9.

A 60 cycle component of voltage was, when required, superimposed on the d-c value of either the plate voltage or the grid voltage. Thus either voltage could be "swept", or varied, for presentation as one coordinate of a two

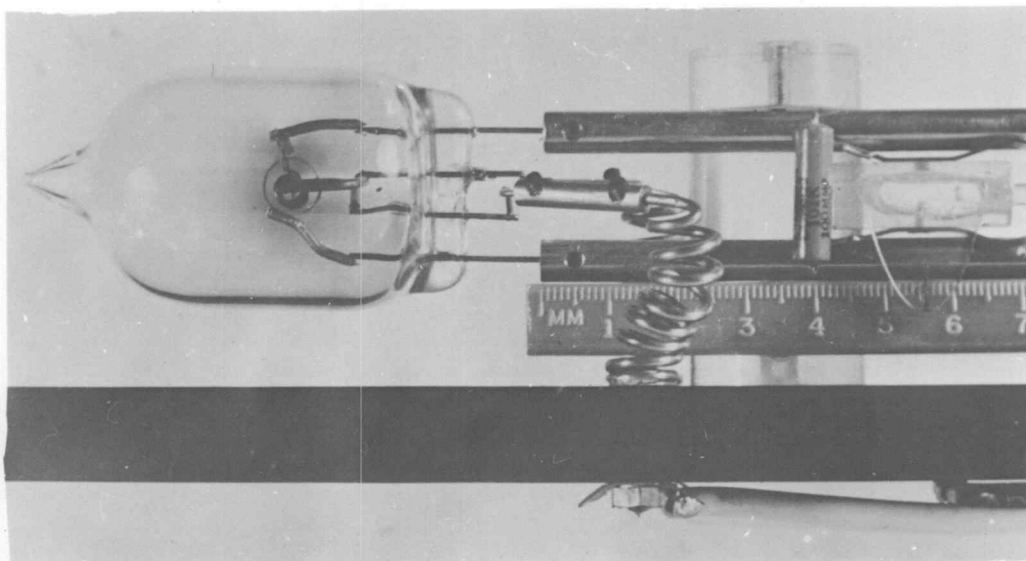


Figure 3 TUBE CONNECTION TO TUNING LINES

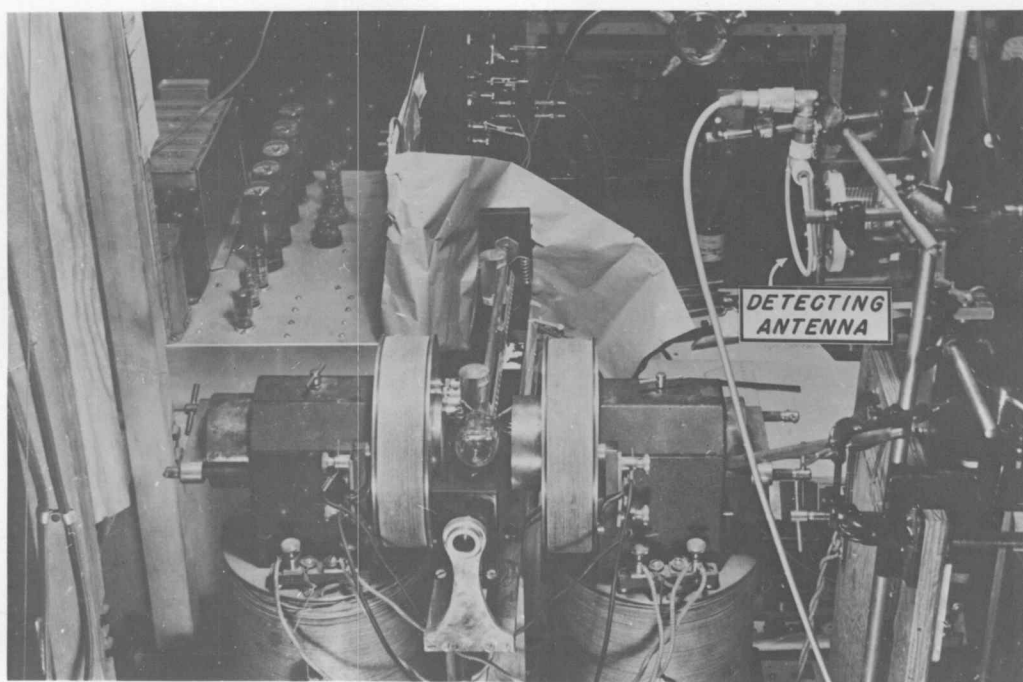


Figure 4 TUBE POSITION BETWEEN MAGNET POLES

dimensional plot on the screen of an oscilloscope. It was also possible to sweep the magnetic field for the same purpose. However, because of the inductance of the magnet, the field sweep was approximately 90 degrees out of phase with the applied voltage, making it necessary to provide a phase shifting network for use with the oscilloscope.

By means of suitable combinations of sweep voltages and dependent variables the following oscilloscope presentations were possible: Plate current as a function of plate potential, grid current as a function of grid potential, plate current as a function of magnetic field, grid current as a function of magnetic field and output as a function of plate potential, grid potential, or magnetic field.

An untuned detector-amplifier was provided to indicate the existence of oscillations. The antenna for the untuned detector consisted of a loop of wire mounted near the General Radio Type 758-A absorption wave meter which was used for rough frequency measurements. This arrangement can be seen in the upper right hand corner of Figure 4. A General Radio Type 720-A heterodyne frequency meter was used for more precise measurements of frequency. Its antenna was extended to the vicinity of the tuning lines by means of a piece of wire. The output of this meter was connected to the Y plates of the oscilloscope, in parallel with the output of the detector-amplifier. This

combination provided an oscilloscope presentation which showed any oscillation present, and in addition allowed indication of the exact frequency at any part of the oscilloscope pattern. Two oscillograms are presented in Figure 5 to show the appearance of the resulting trace.

To determine the effect of the section of tuning lines located on the power supply side of the shorting capacitor, an additional shorting capacitor was added at the power supply connection points. This can be seen in Figure 6 which also shows the paper-backed metal foil which was found necessary for shielding the equipment from the effects of the movements of the operator. Figure 7 is a picture of the experimental apparatus; Figure 8, a combination block and circuit diagram indicating the electrical connections of the equipment.

For determining the effect of the magnetic field on the operating characteristics of the tube a General Radio Type 361-B vacuum tube bridge was used. Fixed operating potentials were supplied by batteries; a Jackson Type audio frequency oscillator provided the a-c signal. A Ballantine Type 300 vacuum tube voltmeter was used as the bridge null indicator. Because of the need for small amplitude test signals and because of the noise and hum levels which prevailed, it was necessary to put a parallel circuit, resonant to the test signal frequency, across the terminals of the vacuum tube voltmeter. As an additional null

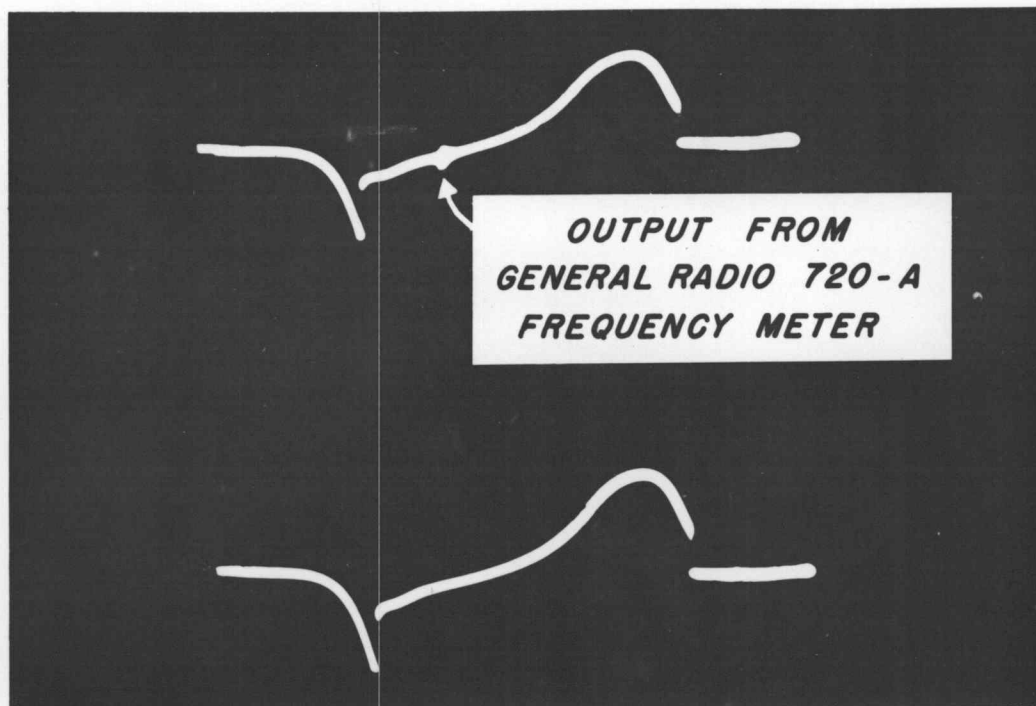


Figure 5 **FREQUENCY INDICATION**

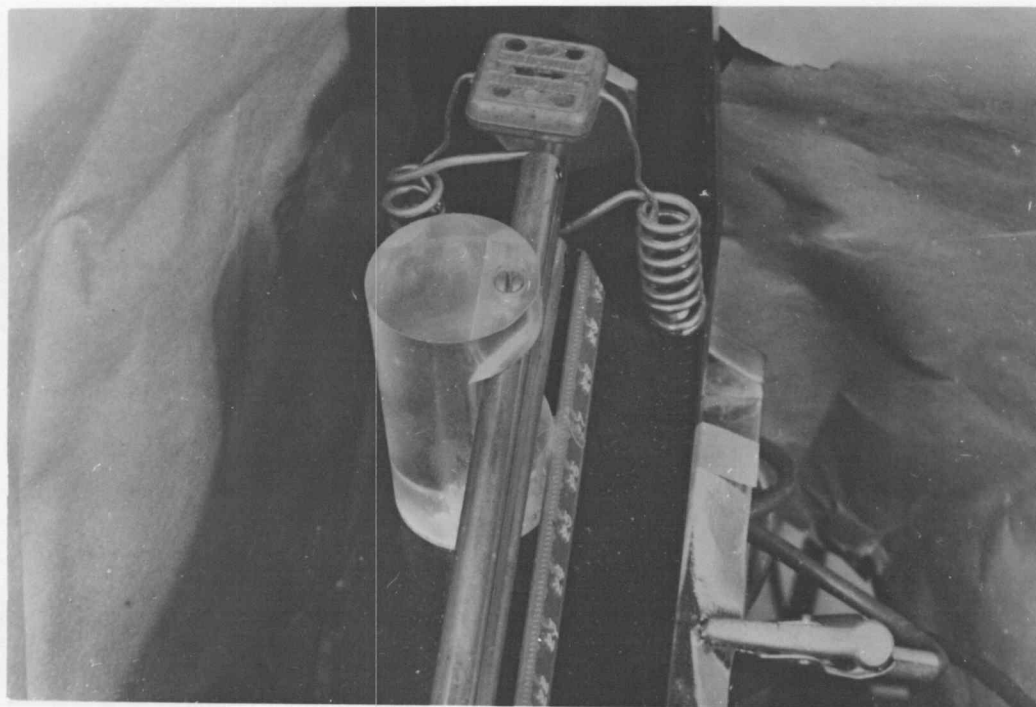


Figure 6 **LINE END SHORTING CAPACITOR**

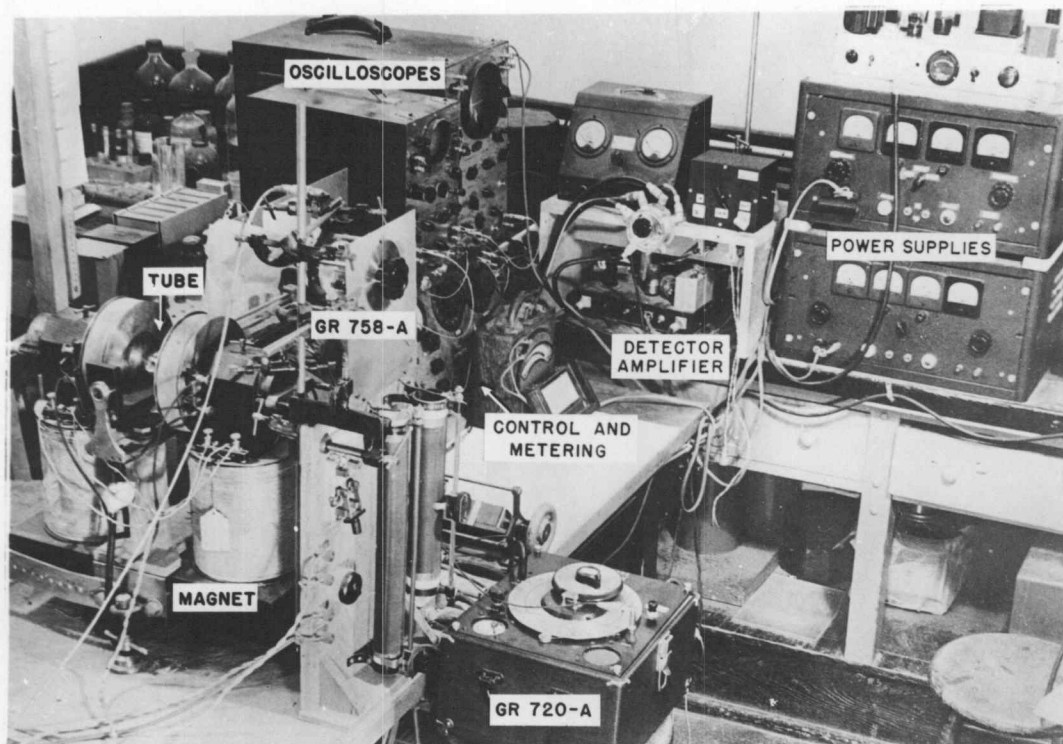


Figure 7 OPERATING POSITION

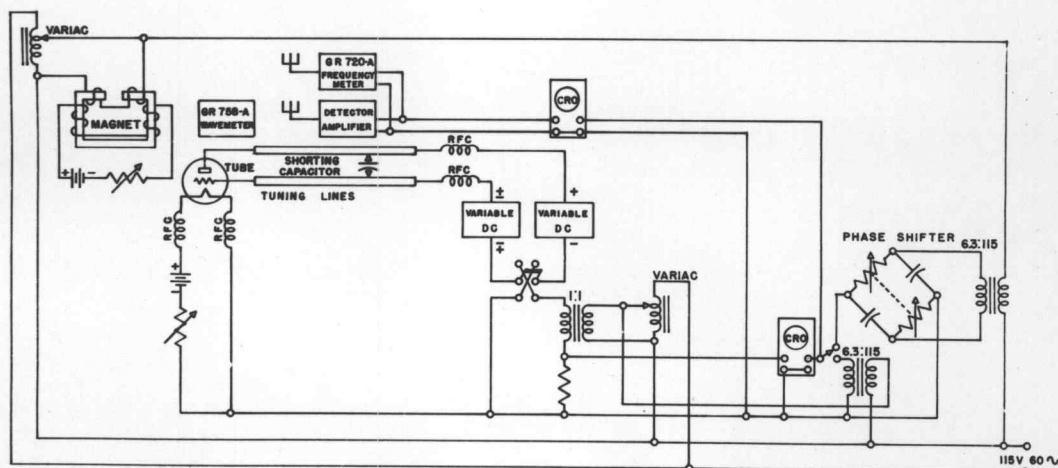
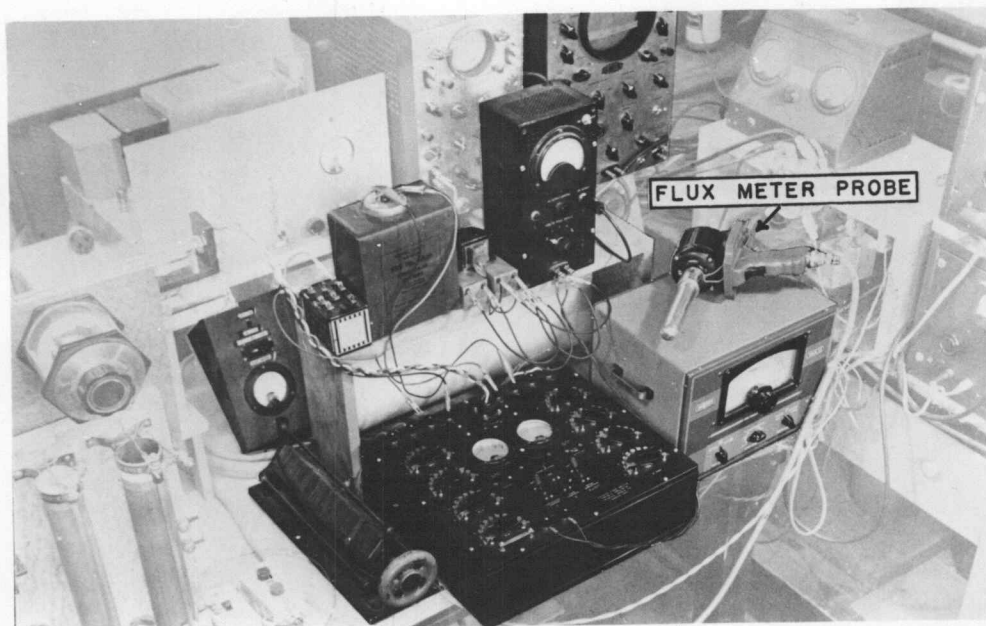


Figure 8 CIRCUIT DIAGRAM

indication the signal at the terminals of the vacuum tube voltmeter was continuously monitored on a cathode ray oscilloscope. The connections to the bridge, the bridge circuits used, and a photograph of the equipment are shown in Figure 9.

For obtaining the potential distribution within the tube a scaled model of a cylindrical segment of the tube was placed in an electrolytic tank. Voltages from the Jackson audio frequency oscillator were applied to the tube elements and the resulting potential distribution was determined by a movable probe connected to the Ballantine vacuum tube voltmeter. Photographs of the equipment and probe, and a sketch of the circuit are found in Figure 10.



Apparatus

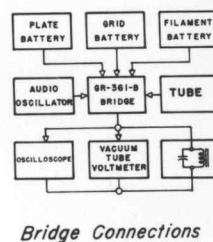
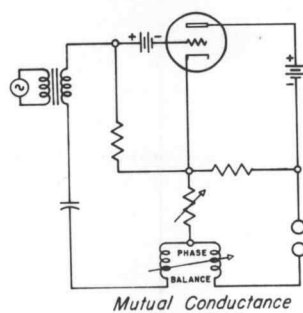
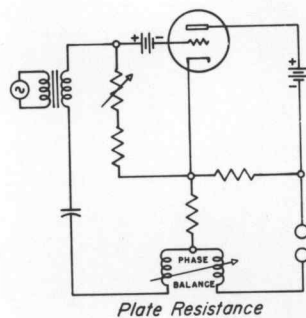
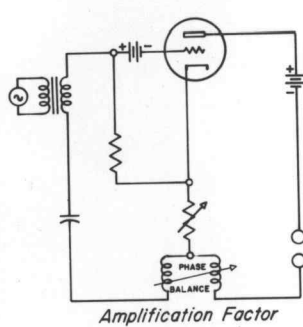
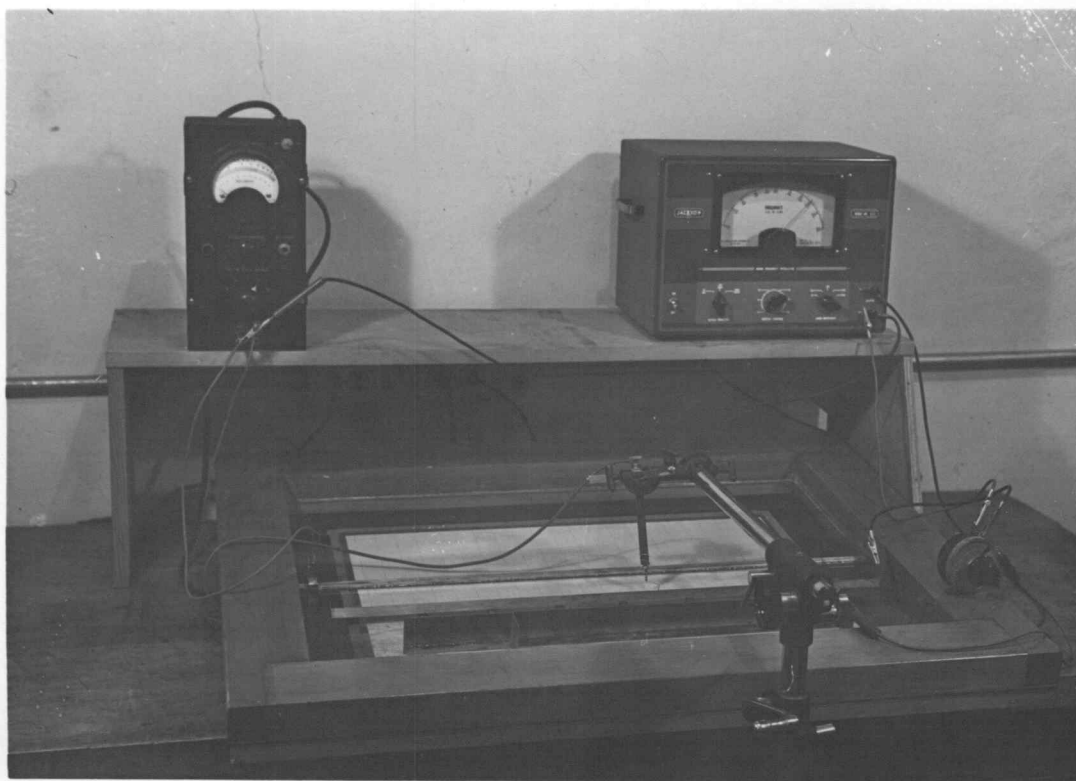
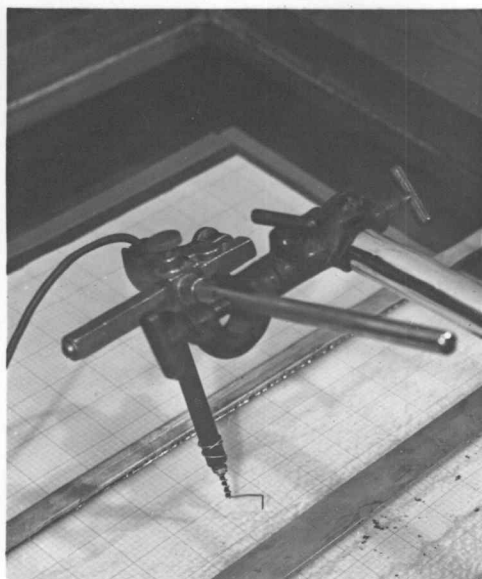


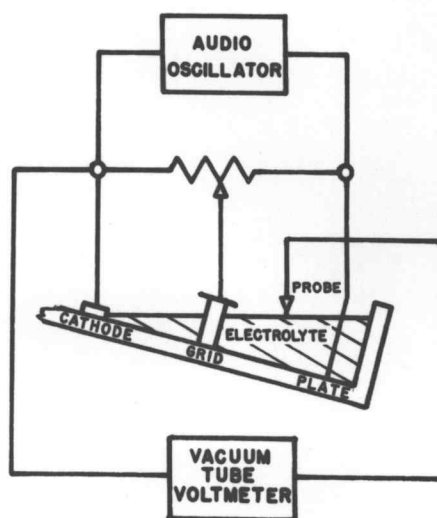
Figure 9 TUBE CHARACTERISTICS EQUIPMENT



Apparatus



Probe



Circuit

Figure 10 ELECTROLYTIC TANK

EXPERIMENTAL INVESTIGATION

The experiments reported herein were conducted in an attempt to determine the extent and cause of the frequency improvement which could be brought about by applying a magnetic field to a triode oscillator.

Data were taken to show those combinations of line-setting and magnetic field which permitted oscillation for all combinations of the other independent variables indicated in Table I. The resulting curves are shown in Figures 11, 12, and 13.

TABLE I

Variable	Lower Limit	Interval	Upper Limit
Plate Voltage	100 Volts	100 Volts	300 Volts
Grid Voltage	-10 Volts	10 Volts	40 Volts
Filament Current	3.8 Amp.	0.1 Amp.	4.6 Amp.
Magnetic Flux Density	0 webers/m ²	Continuously	0.03 webers/m ²
Tuning Line	0 cm.	Continuously	30 cm.

Independent Variables

Oscillograms of grid current and plate current as functions of magnetic field for the values of grid voltage and plate voltage given in Table I, for representative values of filament current are shown in Figures 14 and 15.

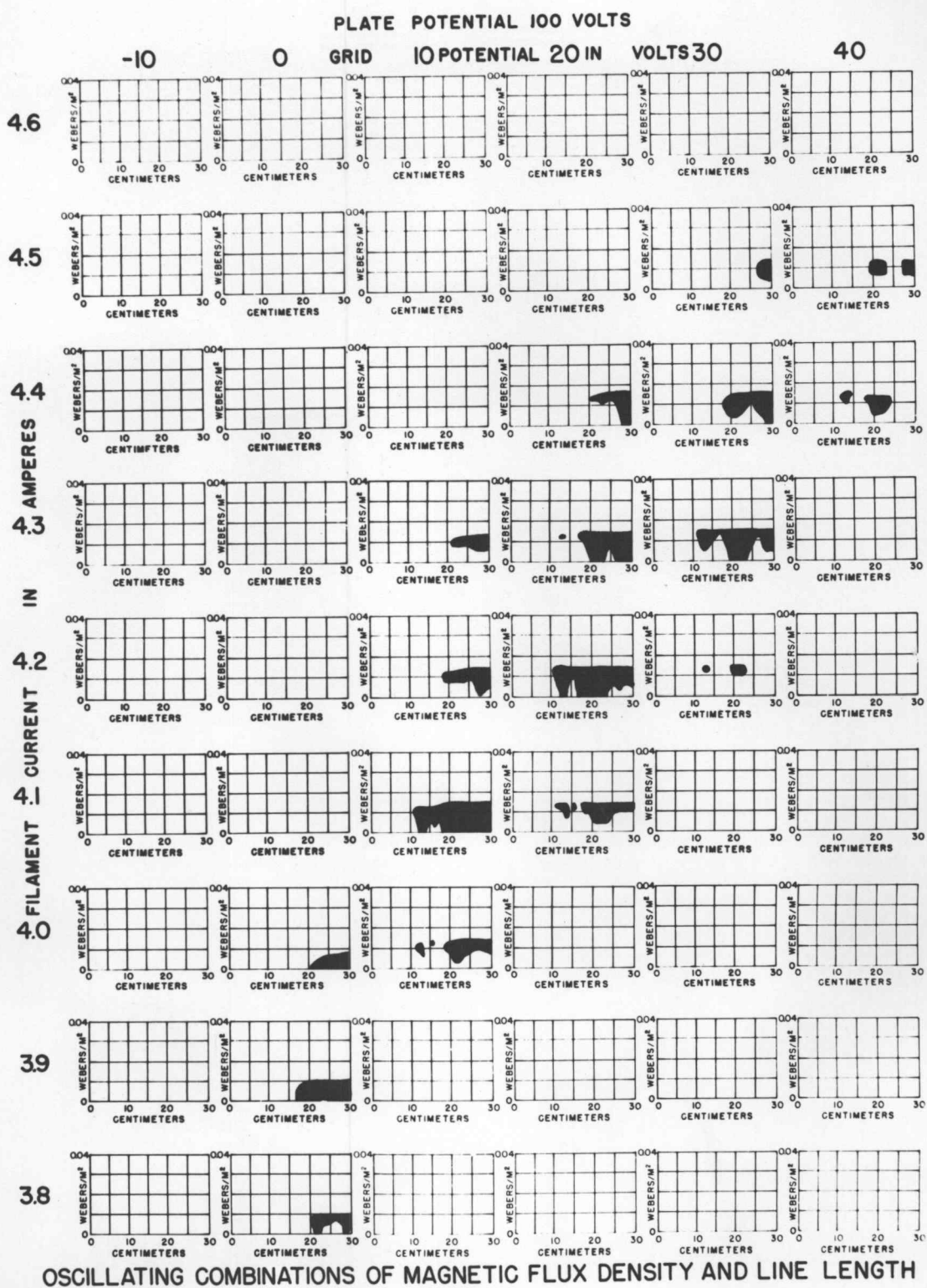


Figure 11

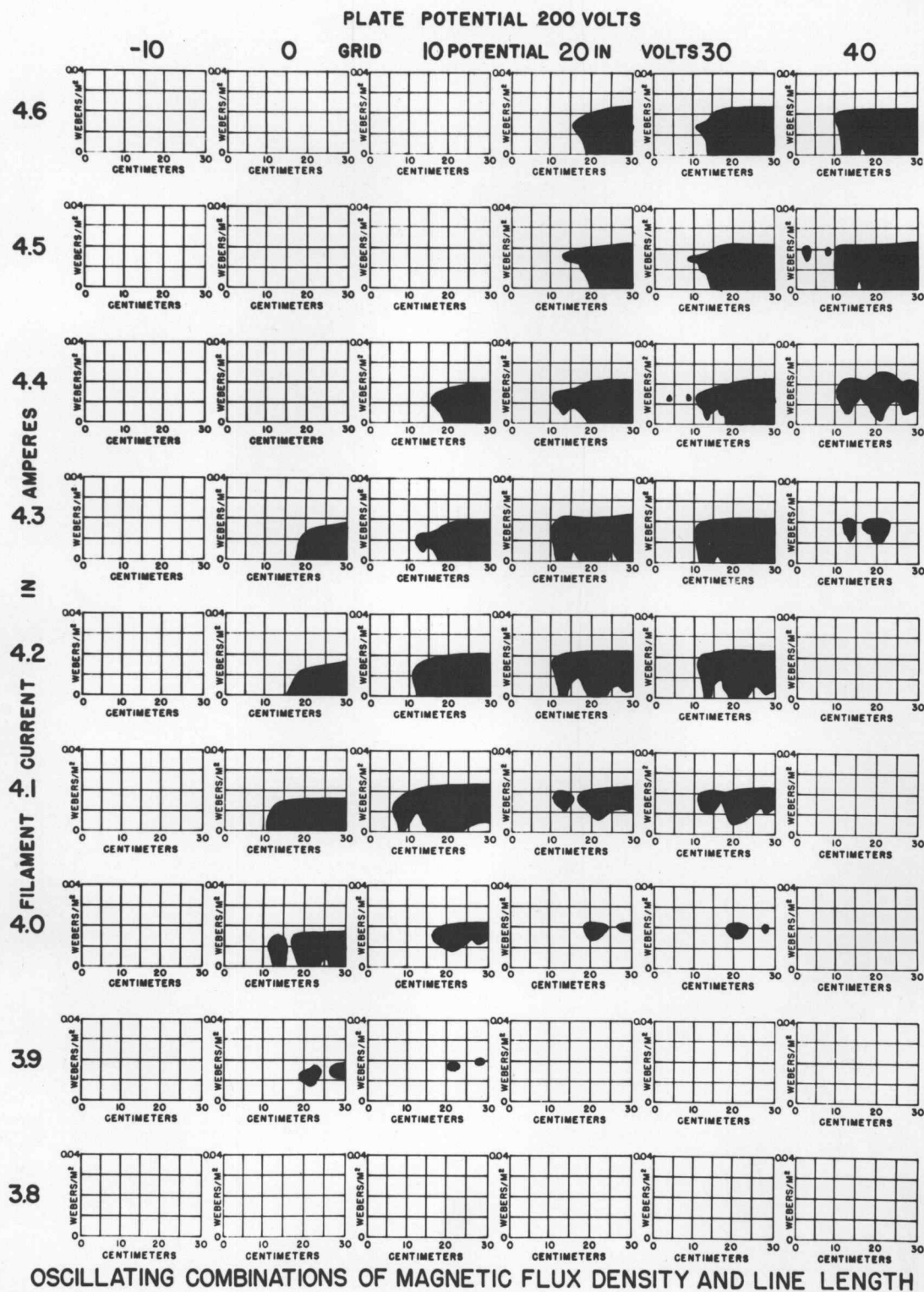


Figure 12

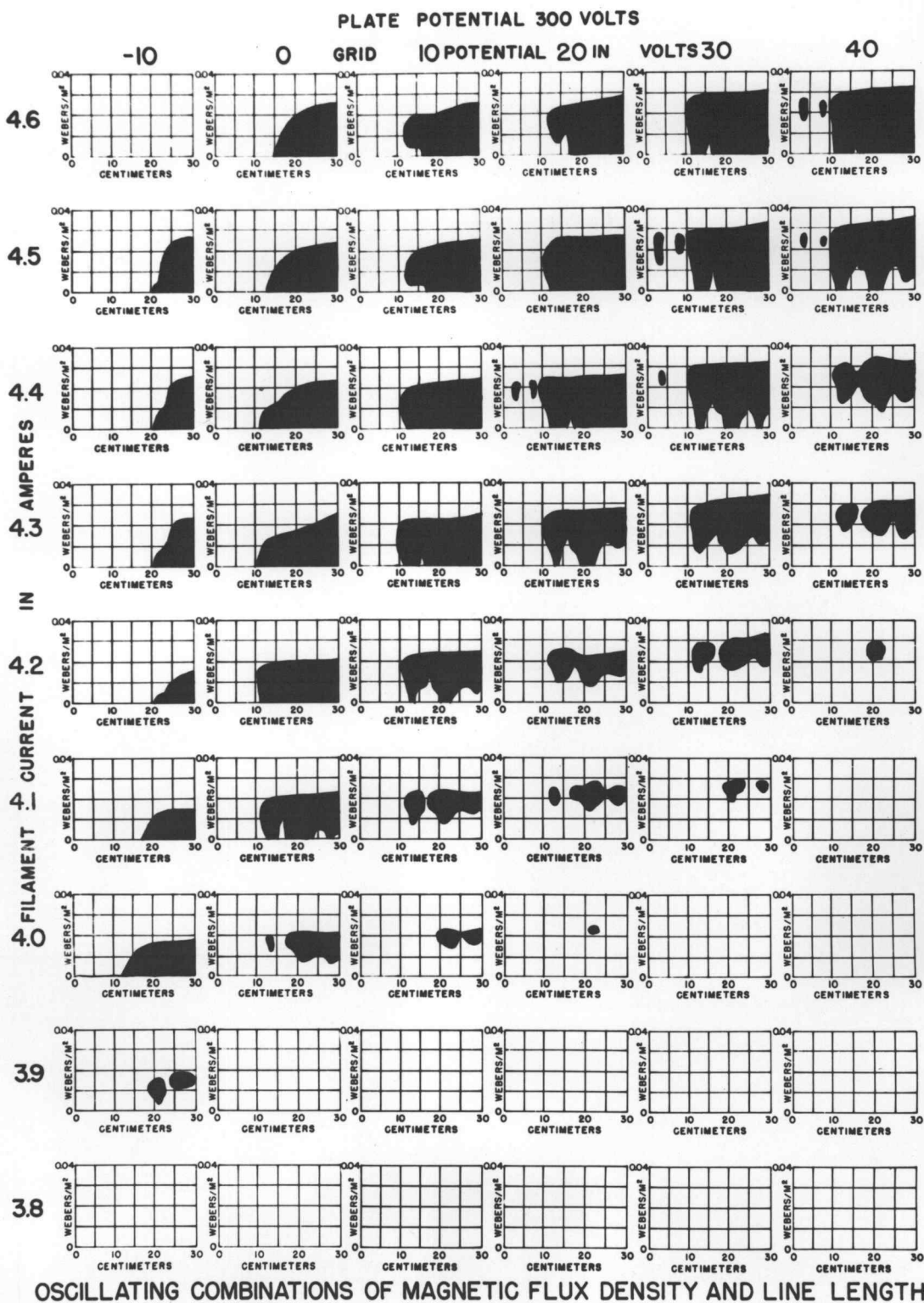


Figure 13

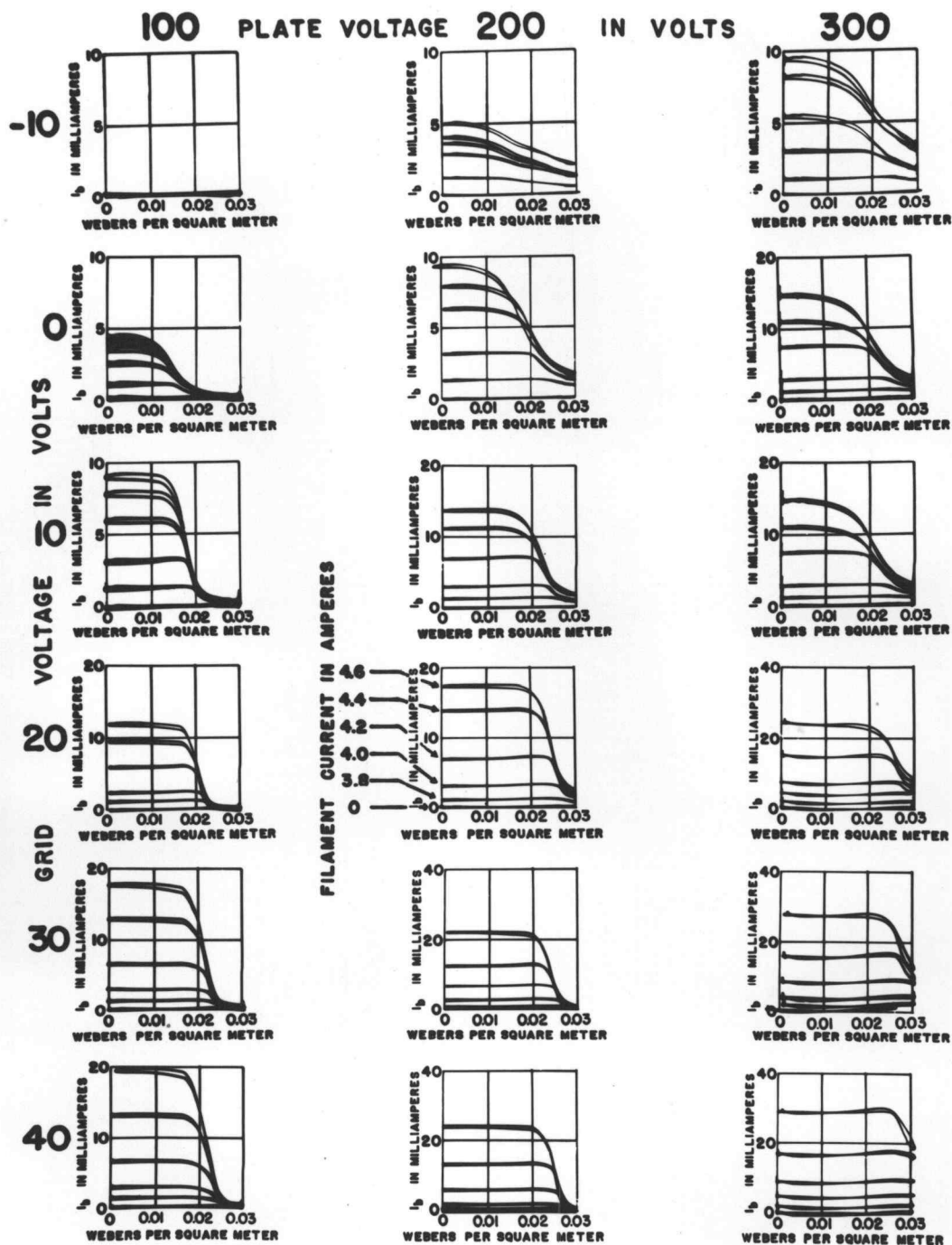
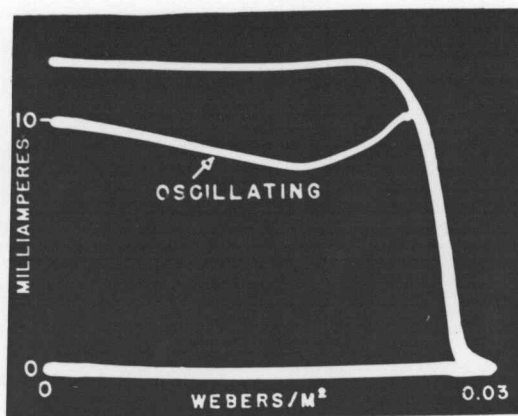


Figure 15

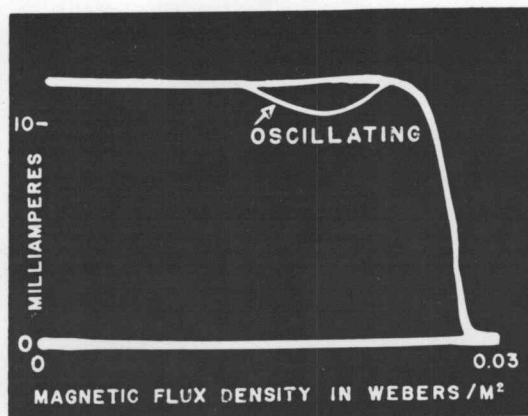
These oscillograms were taken with the tuning lines set at a position which prevented oscillation. To find the effect of oscillation on grid and plate current, the shorting capacitor was shifted to two other positions on the line. For one combination of grid potential, plate potential and filament current, Figure 16-A shows the effect on tube currents of a low frequency oscillation which could be obtained with no magnetic field. Figure 16-B shows, for the same tube potentials, the effect of a high frequency oscillation that existed only when the tube was in a magnetic field.

Since the position of the line-shortening condenser determines the frequency of the oscillator and is easily read, the lengths of the resonant lines have been used throughout this thesis instead of frequency. The relationship between line length and frequency is shown in Figure 17.

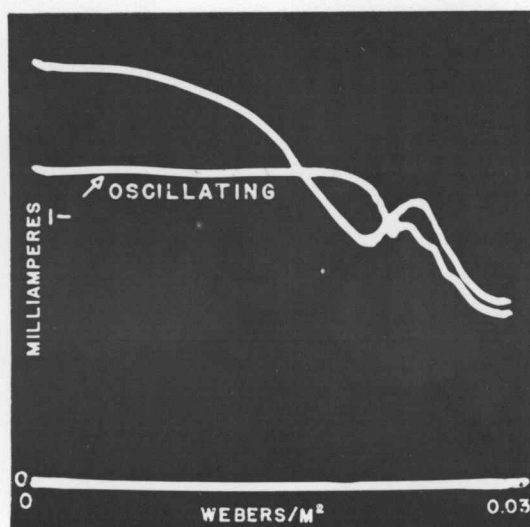
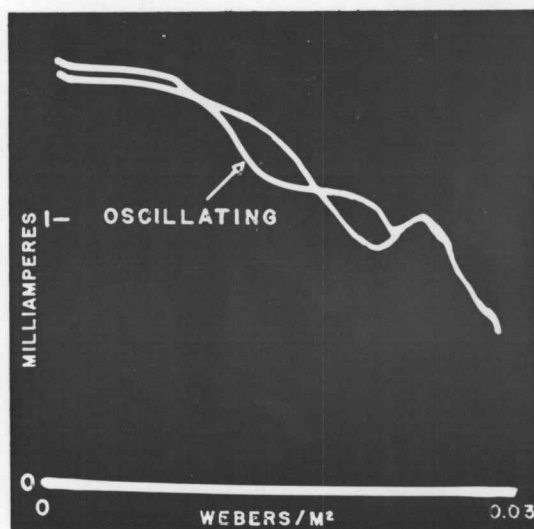
In order to indicate the magnitude of frequency variation for fixed tuning-capacitor settings frequency contours at 10 mc. intervals for combinations of line-setting and magnetic field permitting oscillation are presented in Figure 18. Figure 17 shows curves of wavelength and frequency versus magnetic field plotted from the data of Figure 18. The position of the resonant shorting bar was read by means of the pointer and centimeter scale shown in Figure 3.

*Plate Current*

A
PLATE POTENTIAL 200 V
GRID POTENTIAL 30 V
FILAMENT CURRENT 4.4 A
LINE SETTING 21 CM

*Plate Current*

B
PLATE POTENTIAL 200 V
GRID POTENTIAL 30 V
FILAMENT CURRENT 4.4 A
LINE SETTING 3.5 CM

*Grid Current**Grid Current*

**Figure 16 EFFECT OF OSCILLATION ON
 GRID AND PLATE CURRENTS**

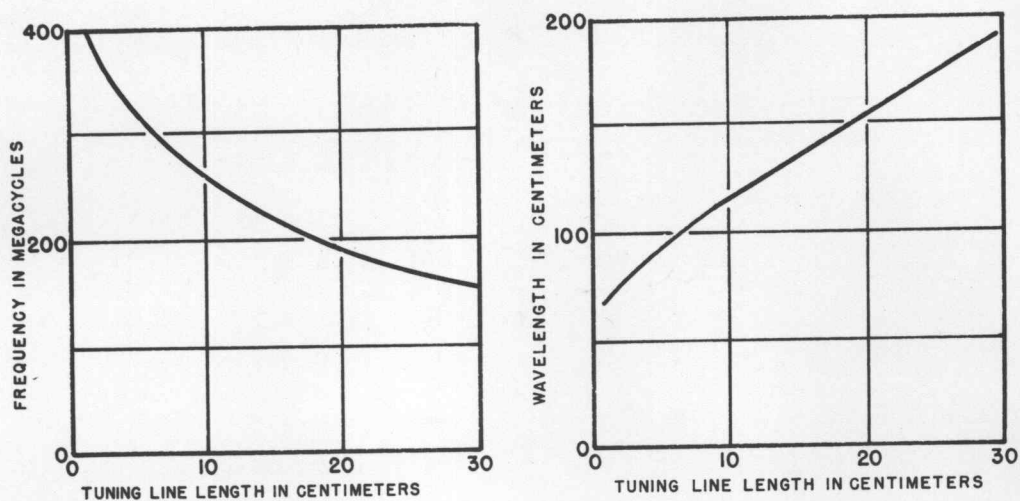


Figure 17 FREQUENCY AND WAVELENGTH VERSUS
LINE SETTING

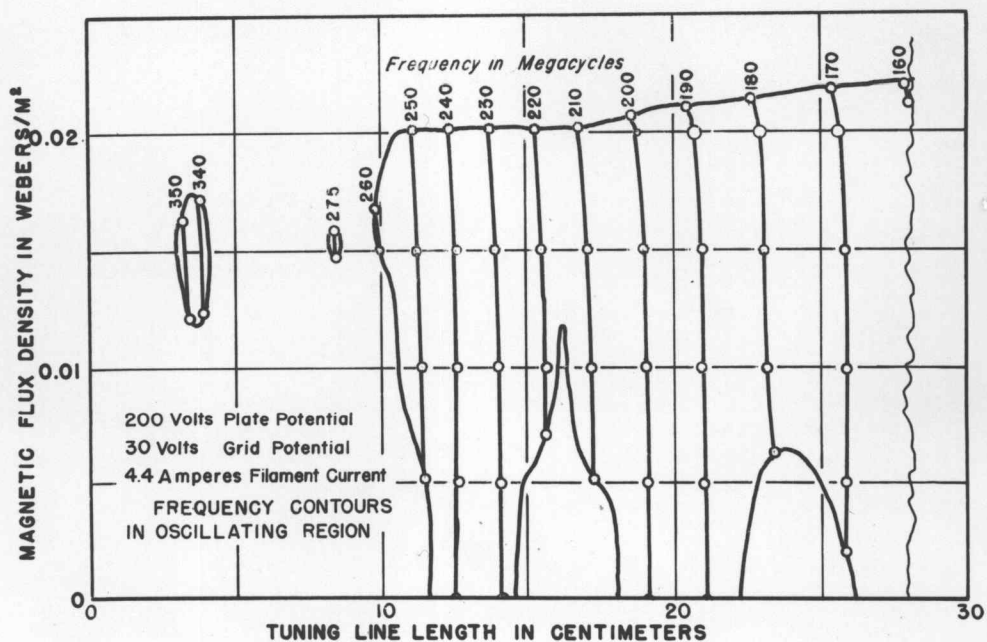


Figure 18 FREQUENCY CONTOURS

Using a vacuum tube bridge the characteristics of the tube were found as functions of magnetic field for values of grid and plate potential which would give typical negative grid operation. The resulting values of amplification factor, mutual conductance, plate resistance, and plate current are plotted in Figure 19.

The tube potential distributions which were found by means of the electrolytic tank are shown in the section on calculations together with the transit times which were computed from them.

With the shorting capacitor across the power supply end of the lines, as shown in Figure 6, data were taken showing the combinations of line-settings and magnetic flux densities giving oscillations for a given combination of tube element potentials and filament current. These data are shown in Figure 20 together with corresponding data resulting from the same combination of tube conditions but with no line-end shorting capacitor.

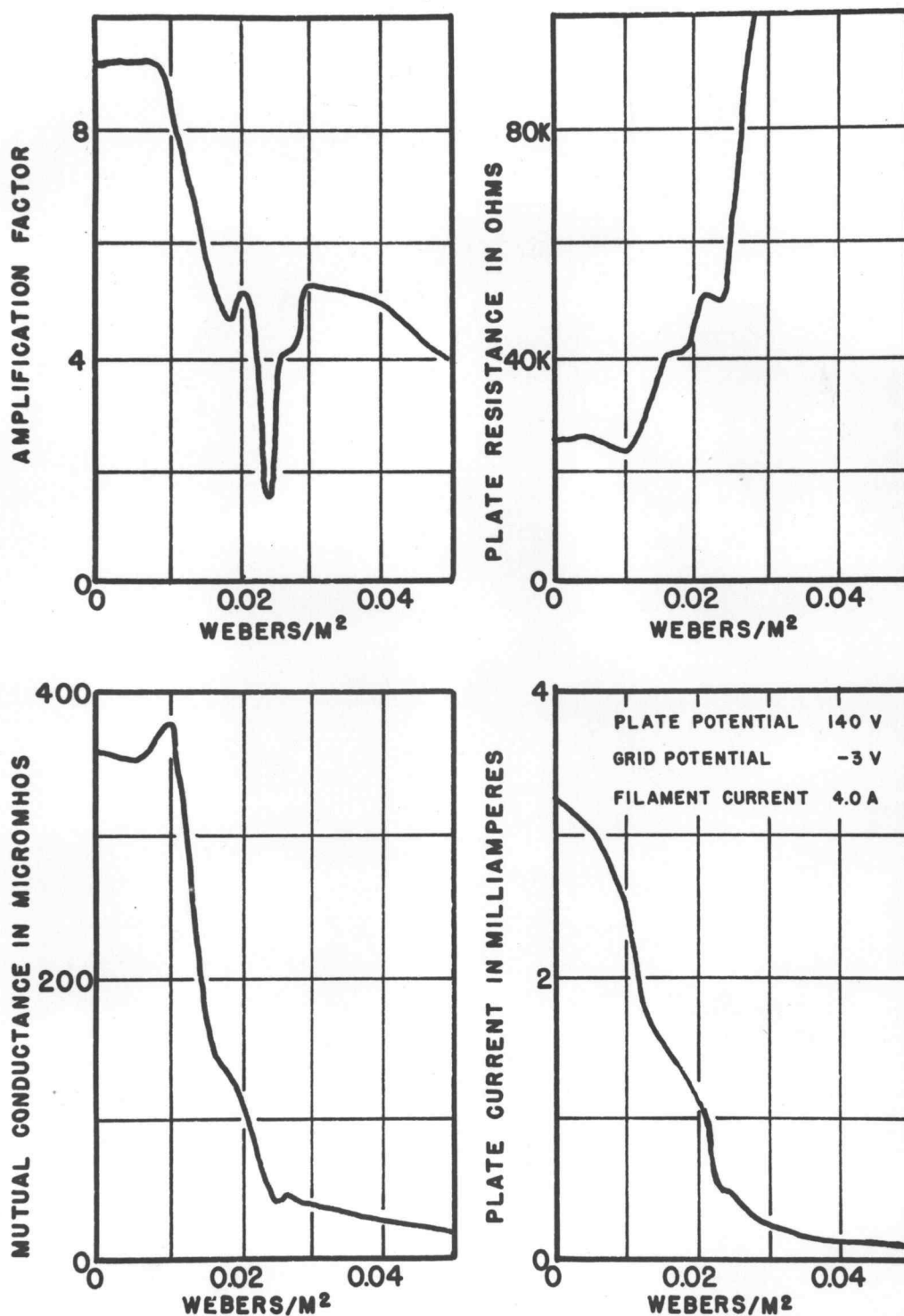
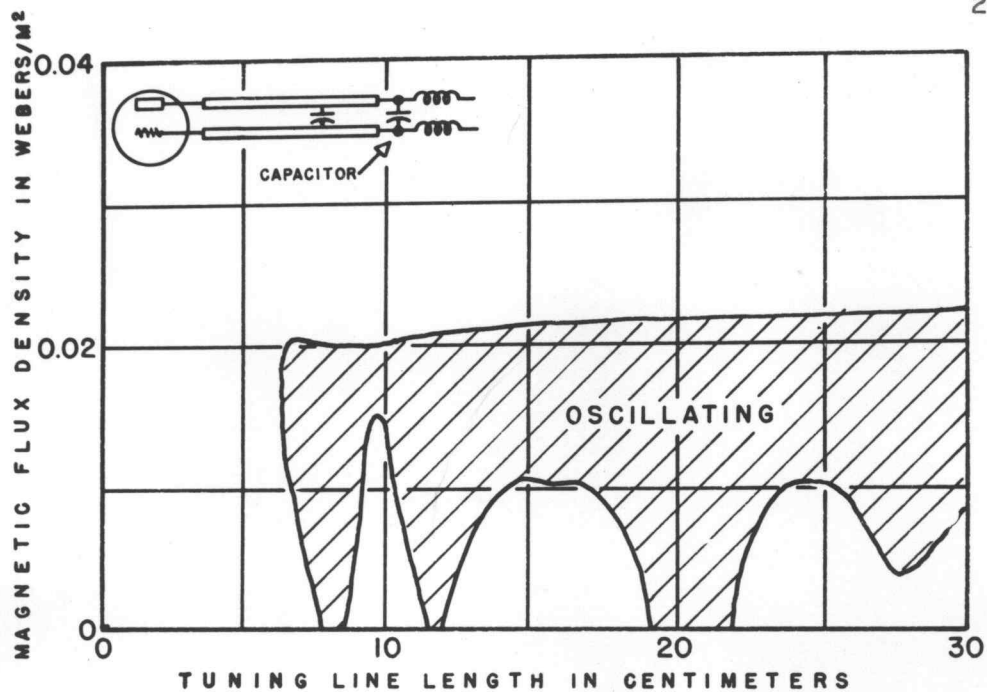
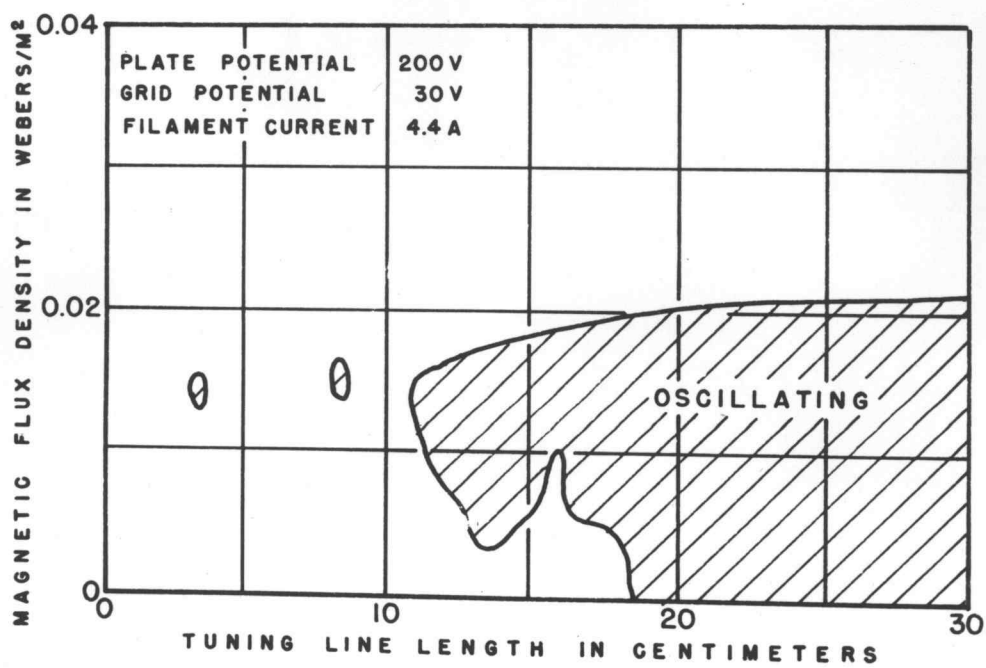


Figure 19 TUBE CHARACTERISTICS VERSUS MAGNETIC FLUX DENSITY



A. With Capacitor



B. Without Capacitor

Figure 20 EFFECT OF LINE-END SHORTING CAPACITOR

CALCULATIONS

It was thought that the observed increase in the high frequency oscillation limit brought about by the use of a magnetic field, was in some way a function of the transit time of the electrons in the tube.

In order to investigate these transit time effects, electron paths were calculated for certain somewhat idealized conditions of operation. To simplify the equation for electron motion it was assumed that the tube was cylindrically symmetrical. This was accomplished by assuming the grid structure to consist of a series of equipotential toroids rather than a helix. For the solution of the electron motion equation it was necessary that the potential distribution within the tube be known. The derivation of a mathematical solution for this potential distribution would be quite difficult. However, a sufficiently close approximation was obtained by the use of an electrolytic tank and a scaled model of a tube sector, Figure 10.

Since the paths of the electrons which would be most likely to reach the plate and grid, were of greatest interest, the potentials for these regions were measured. The plate is most likely to receive those electrons which pass midway between two grid wires while the grid is most likely to receive those traveling toward the center of a grid wire. Potential distributions along these two radial lines were

investigated and electron transit times calculated numerically from the results. The potential distributions and transit times which resulted from the application of the values in Table II are shown in Figure 21.

TABLE II

Plate Potential Volts	Grid Potential Volts	Magnetic Flux Density Webers/m ²
200	0	0
200	0	0
200	30	0
200	30	0.015
200	30	0.020

Parameters for calculated electron paths

From discussions of space charge effects for triodes (4, p.514), and for magnetrons (4, p.648), it seemed reasonable to assume that the actual operating conditions within the tube were such that a virtual cathode surface would exist somewhere between the cathode and the plate surfaces. A linear potential drop from this virtual cathode to the plate structure also seemed to be a logical approximation. Substituting the potential distribution assumed to exist under space charge conditions, into the equation for electron motion, electron paths were

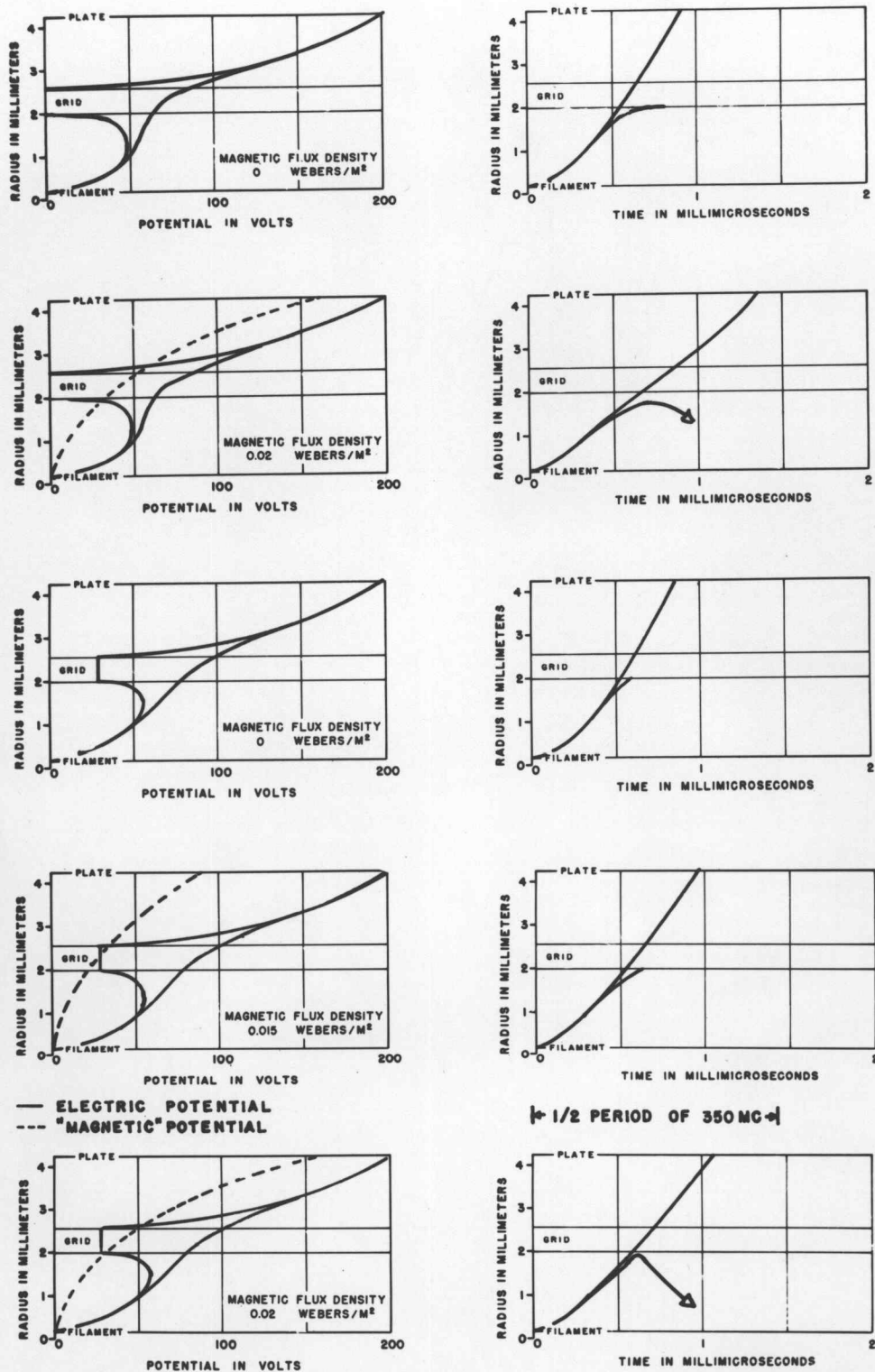


Figure 21 ELECTRON TRANSIT TIMES, POTENTIAL MEASURED

calculated as functions of the variables indicated in Table II. The potential distributions and resulting transit times are shown in Figure 22. The derivation of the electron motion equation which was used for the transit time calculations, and a discussion of its parameters, including measured and assumed potential functions, is given as Appendix I.

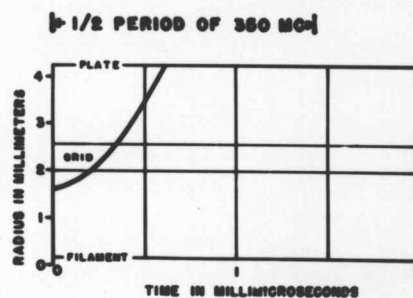
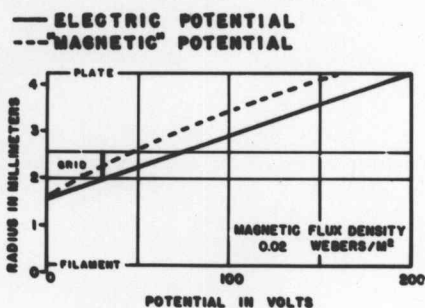
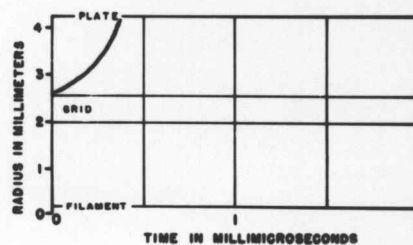
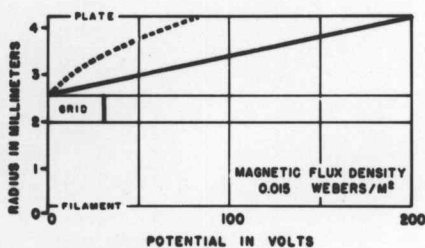
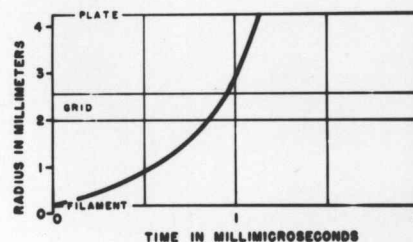
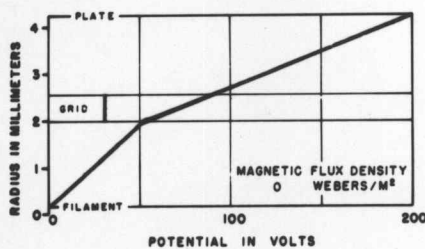
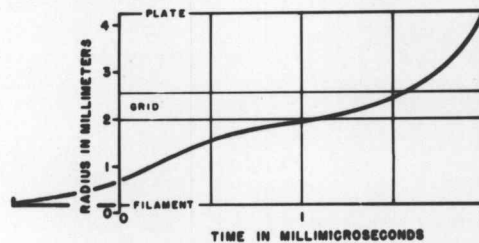
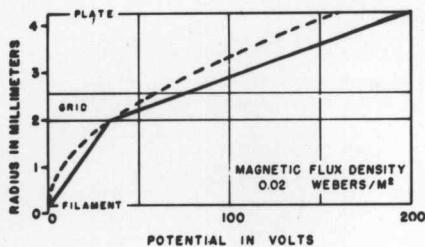
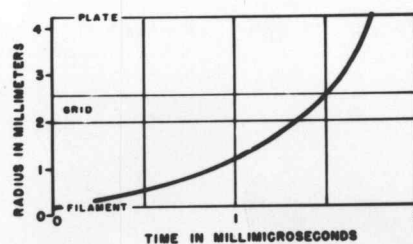
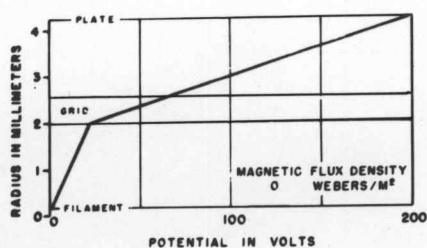


Figure 22 ELECTRON TRANSIT TIMES, POTENTIAL ASSUMED

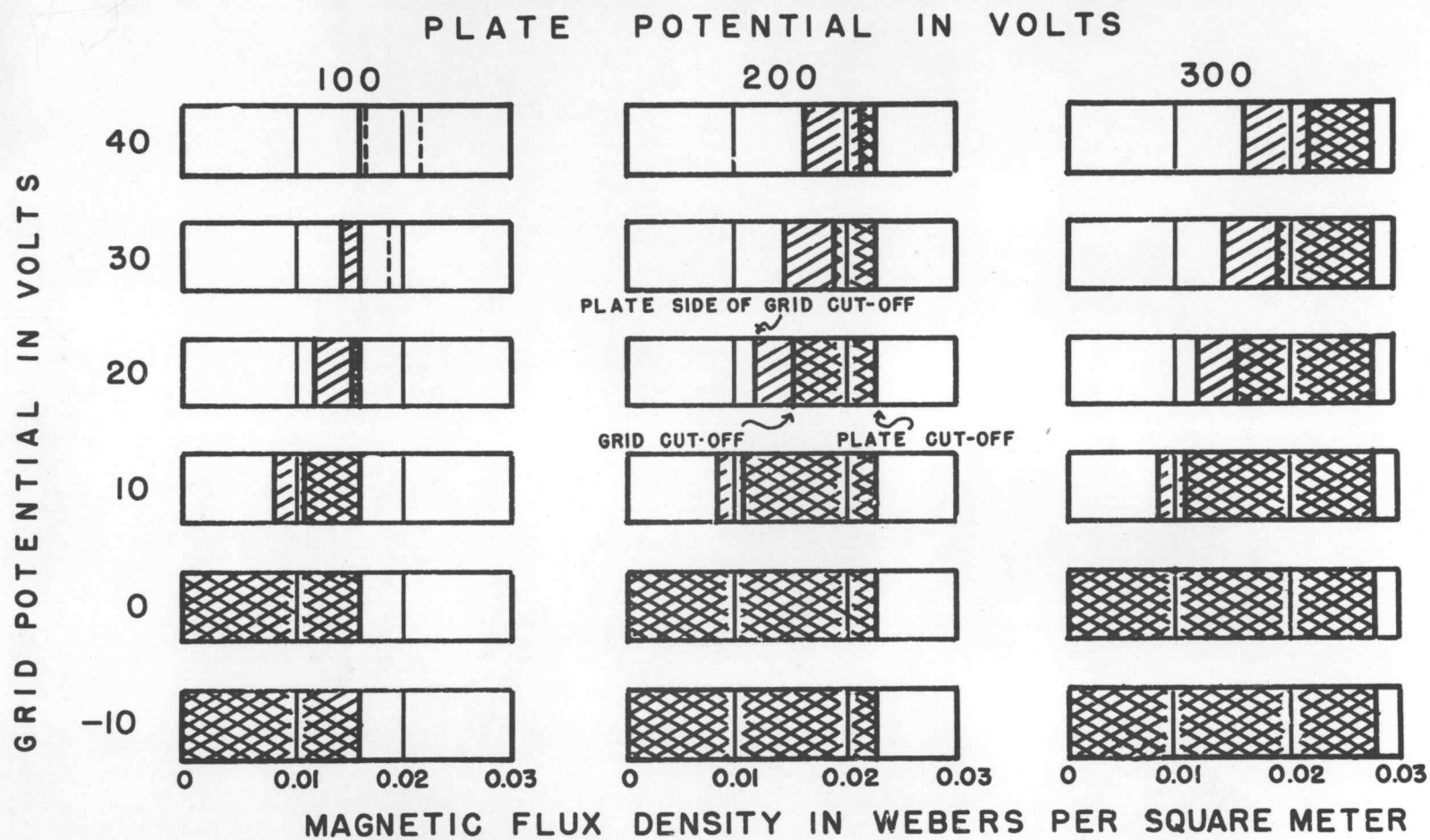
CONCLUSIONS

Before investigating the theory of the effect of magnetic field on the upper frequency limit of oscillation, it is desirable to discuss several points that are evident from the data but which have no particular effect on the theory. These should be explained in order to prevent their appearing as possible contradictions to the theory.

It can be seen in Figures 11, 12, 13, and others, that there are certain values of line-setting at which it is exceedingly difficult to obtain oscillations. It was this condition which prompted the use of the shorting condenser on the back section of the tuning lines. However, as can be seen in Figure 20, the positions of the unfavored oscillation regions were essentially unchanged. Since there was no apparent change in unfavored frequencies as a function of magnetic field, it was assumed that the trouble was caused by some circuit phenomenon. A lumped capacitance-lumped inductance type of resonant circuit has, theoretically, only one resonant frequency, while a distributed impedance circuit, e.g., resonant lines, exhibits a fundamental resonance frequency, and also harmonics of this frequency. The favored oscillations appeared to be harmonics of a fundamental wavelength of approximately 680 cm. and the unfavored oscillations, harmonics of a 640 cm. fundamental. From this it seems that the disturbing

element was probably a tuned circuit of the distributed impedance type. There were several such possibilities which had not been considered at the time that the equipment was dismantled and therefore have not been checked. The first of these is the grid of the tube itself. This consisted of a shorted helix, with an inductance of approximately 2 microhenries. This would require a capacitance of approximately 10 micromicrofarads for resonance at the observed fundamental. The grid to plate capacitance of the tube was approximately 2 micromicrofarads and the distributed capacitance of the grid should be of the same order of magnitude. A change in grid structure should determine whether or not this might be the cause of the trouble. As another possibility, the filament leads were in such a position that they might have been coupling out energy and producing the observed effects. It is also possible that some other part of the system, as yet unsuspected, might be responsible. However, although this frequency-selective oscillation-rejection is a disturbing effect, it seems sufficiently evident that the variables under investigation are not at fault and that the data, as observed, present ample evidence of the improvement brought about by the magnetic field.

Calculated values of the magnetic fields necessary for both grid and plate cut-off, for the voltages used, are shown in Figure 23. Because of its thickness, the grid has



REGIONS FAVORING OSCILLATION IMPROVEMENT

Figure 23

a range of cut-off values. This range is shown by the single cross-hatched areas in the chart. The double cross-hatched areas indicate that the grid is completely cut off but that the plate is not. Since the actual grid and plate cut-off values are not as sharp as would be indicated mathematically, the tube is capable of operating over a somewhat wider range of conditions than that shown in Figure 23. This can be attributed to a number of effects. The tube elements themselves are not as perfectly constructed as the equations assume. Emission and space charge effects tend to produce variations in electron velocity. Also, electrons which pass through different portions of the tube are subjected to different potential conditions because of the arrangement of tube elements.

From the observations and calculations which were made, it has been established that there is an appreciable improvement in the upper frequency limit of the triode oscillator which was examined. An examination of the information obtained from these data and a discussion of some possible causes of the frequency and amplitude improvements observed, can now be undertaken.

Several things are evident from Figures 11, 12, and 13, which show conditions necessary for oscillation, Figures 14 and 15 presenting element currents versus magnetic field, and Figure 23 which shows the calculated values of magnetic field for grid and plate cut-off.

First it can be seen that positive grid potential is necessary for obtaining high frequency oscillations. Also, for each combination of grid and plate potential there is an optimum value of filament current which seems to be proportional to the product of grid and plate voltages. The maximum frequency which can be reached seems to depend on this optimum filament current whether a magnetic field is present or not. It can also be seen that the high frequency performance falls off with the higher values of filament current. The best conditions of frequency improvement seem to be centered about the values of magnetic field which are very near those necessary for grid cut-off, especially for those conditions in which this value of field is considerably less than that necessary for plate cut-off.

Little has been found in the literature as to the relationship between cathode emission and tube operation. Some probable effects seem reasonable however. As the emission increases, the space charge increases, and for large values of emission the potential in the grid-plate space would probably be decreased by the space charge to such an extent that the grid-plate transit time would be materially increased. This could possibly result in longer cathode-plate transit time than that resulting from conditions of little or no space charge. This would explain the decrease in high frequency operation which was observed

with high filament currents.

The magnetic field also tends to increase the space charge, but in a somewhat different manner. With the grid operating near magnetic cut-off potential, electrons will be kept in the grid region for long periods of time thus producing a dense electron cloud in the vicinity of the grid. Because of the magnetic field, this cloud will rotate as a cylinder coaxial with the tube and will appear, to the other tube elements, to be the surface of a virtual cathode. The effects of the magnetic field will be such that the boundary between this space charge cloud and the relatively space-charge-free region beyond, will be much sharper than would be the case for operation without the magnetic field. Also, because of the magnetic field, the density of the electron cloud will be greater than that normally existing. This combination will cause a steep potential gradient in the grid region thereby permitting rapid acceleration of electrons between the grid and plate. The space charge cloud will shield the cathode from the grid and act as the emitting surface to such an extent that the transit time can be considered as the time required for an electron to travel from the surface of the virtual cathode to the plate. This transit time will be much shorter than the cathode-plate time with no magnetic field, because of the shorter distance and steeper potential gradient. These effects can be seen in Figure 22. As the

magnetic field is increased the electron density in the grid region is increased, and with additional field, the virtual cathode is moved back toward the true cathode until the transit time is again too long for the higher frequencies of oscillation. The best operation can be expected for those conditions giving the sharpest virtual cathode boundary and the closest grid-to-virtual-cathode spacing. It can reasonably be expected that these conditions are satisfied by certain combinations of potentials, emissions, and magnetic fields that produce optimum values of emission current and approximate grid cut-off, and provide values of plate potential that are as large as possible for the tube being used.

With no magnetic field the grid conduction current for positive grid voltage is in phase with the grid current thus causing an additional component of grid loss. The magnetic field helps this condition by decreasing the grid current, especially for values of magnetic field approximating grid cut-off.

In summing up the causes of the improvement in high frequency operation it appears that with the proper magnetic field the space charge is increased but is concentrated into a region that changes the grid-cathode space and the grid-plate potential gradient in such a way that the cathode-plate transit time is materially reduced. The plots in Figure 22 which indicate this improvement are at

best only rough estimates but the assumptions on which they are based are close enough to known facts relative to the operation of tubes to appear somewhat reasonable. The transit time differences might not be so pronounced as Figure 22 indicates but they might easily be comparable to the values of frequency improvement observed and should be greater than the transit time differences shown in Figure 21 for the same conditions assuming no space charge.

Further study should be made, experimentally and mathematically, of space charge and cathode emission effects, to confirm or disprove the assumptions made herein. Experiments should be conducted with different tube geometries and oscillator circuits to see if the advantages realized with this tube and circuit can be duplicated with others.

With the tube used, an appreciable improvement in frequency limit was realized and, if the assumptions about space charge are correct, this improvement would seem to be a result of the effects of magnetic field on space charge magnitude and distribution.

LITERATURE CITED

1. Blewett, John P. and Simon Ramo. High frequency behavior of a space charge rotating in a magnetic field. Physical review 57:635-641. 1940 (Series 2).
2. Gavin, M. R. Triode oscillators for ultra-short wave lengths. The wireless engineer 16:287-296. 1939.
3. Milne, William Edmund. Numerical calculus. Princeton, Princeton University, 1949. 393p.
4. Spangenberg, Karl R. Vacuum tubes. New York, McGraw-Hill, 1948. 860p.
5. Terman, Frederick Emmons. Radio engineers' handbook. New York, McGraw-Hill, 1943. 1019p.
6. Varner, William R. The fourteen systems of units. Second revised. Corvallis, Oregon State College Cooperative Association, 1948. 217p.



ADVANCE BOND

CHAS. L. BROWN

APPENDIXES

APPENDIX I

EQUATION OF ELECTRON MOTION

In order to find the theoretical paths of electrons within the tube, Newton's Second Law of motion was used. In vector form, using the rationalized MKS system of units, this is,

$$(1) \quad \mathbf{F} = m\ddot{\mathbf{R}}$$

\mathbf{F} = vector force on particle in newtons

m = particle mass in kilograms

$\ddot{\mathbf{R}} = \frac{\partial^2 \mathbf{R}}{\partial t^2}$ = vector acceleration of particle in meters/sec²

The significant part of the force on the electron consists of two terms. The first of these is produced by the electric field and is given by:

$$(2) \quad \mathbf{F}_e = -e\mathbf{E}$$

\mathbf{F}_e = vector force on particle in newtons

$-e$ = electron charge in coulombs

\mathbf{E} = vector electric field in volts per meter

The second part of the force comes from the magnetic field and is:

$$(3) \quad \mathbf{F}_m = -e\dot{\mathbf{R}} \times \mathbf{B}$$

\mathbf{F}_m = vector force of particle in newtons

$\dot{\mathbf{R}}$ = vector velocity of particle in meters/sec

\mathbf{B} = vector magnetic field in webers/meter²

B = magnitude of \mathbf{B} in webers/meter²

Combining these terms, a general differential equation for electron motion is obtained:

$$-e(\dot{\mathbf{R}} \times \mathbf{B} + E) = m\ddot{\mathbf{R}}$$

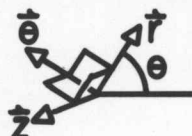
which may for convenience be written:

$$(4) \quad \ddot{\mathbf{R}} + \frac{e}{m}(\dot{\mathbf{R}} \times \mathbf{B} + E) = 0$$

Some simplification can be realized by means of investigating this equation in terms of the cylindrically symmetrical tube used. The usual cylindrical coordinates r , θ , and z are used, with the axis of symmetry of the tube coinciding with the z axis.



A set of unit vectors are determined as follows:



\hat{r} in the direction of increasing r

$\hat{\theta}$ in the direction of increasing θ

\hat{z} in the direction of increasing z

With these coordinates and unit vectors the vector,

$$\mathbf{R}(r, \theta, z)$$

is defined as the position vector of an electron in the tube.

$$(5) \quad R = R(r, \theta, z) = r\vec{r} + z\vec{z}$$

r = radial distance from z axis in meters

z = distance from \vec{r} to origin, along z axis, in meters

then by vector differentiation with respect to time:

$$(6) \quad \dot{R} = \dot{r}\vec{r} + r\dot{\theta}\vec{\theta} + \dot{z}\vec{z}$$

$$\ddot{R} = \begin{cases} \frac{d}{dt}(\dot{r}\vec{r}) = \ddot{r}\vec{r} + \dot{r}\dot{\theta}\vec{\theta} \\ \frac{d}{dt}(r\dot{\theta}\vec{\theta}) = \dot{r}\dot{\theta}\vec{\theta} + r\ddot{\theta}\vec{\theta} - r(\dot{\theta})^2\vec{r} \\ \frac{d}{dt}(\dot{z}\vec{z}) = \ddot{z}\vec{z} \end{cases}$$

or

$$(7) \quad \ddot{R} = [\ddot{r} - r(\dot{\theta})^2]\vec{r} + [2\dot{r}\dot{\theta} + r\ddot{\theta}]\vec{\theta} + \ddot{z}\vec{z}$$

The magnetic flux density, \vec{B} , is applied in the \vec{z} direction only, therefore:

$$(8) \quad \dot{R} \times \vec{B} = \begin{vmatrix} \vec{r} & \vec{\theta} & \vec{z} \\ \dot{r} & r\dot{\theta} & \dot{z} \\ 0 & 0 & B \end{vmatrix} = r\dot{\theta}B\vec{r} - B\dot{r}\vec{\theta}$$

The electric field E is assumed to be in the direction \vec{r} only.

Substituting equations (7) and (8) in equation (4) gives equation (1) in the form

$$(9) \quad (\ddot{r} - r(\dot{\theta})^2 + r\dot{\theta}\frac{Be}{m} + \frac{e}{m}E)\vec{r} + (2\dot{r}\dot{\theta} + r\ddot{\theta} - \frac{Be}{m}\dot{r})\vec{\theta} + \ddot{z}\vec{z} = 0$$

Since the unit vectors chosen form an independent

set, it is necessary that all of their components be 0 in order that the sum be 0. This gives

$$(10) \quad \ddot{r} - r(\dot{\theta})^2 + r\ddot{\theta}\frac{Be}{m} + \frac{e}{m}E = 0$$

$$(11) \quad 2\dot{r}\dot{\theta} + r\ddot{\theta} - \frac{Be}{m}\dot{r} = 0$$

$$(12) \quad \ddot{z} = 0$$

Equation (12) can be easily solved giving:

$$(13) \quad z = \dot{z}_0 t + z_0$$

where

\dot{z}_0 = initial velocity in \hat{z} direction in
meters/sec

z_0 = initial value of z in meters

Equation (11) can be solved for $\dot{\theta}$ as follows:

It can be seen that

$$(14) \quad 2\dot{r}\dot{\theta} + r\ddot{\theta} = \frac{1}{r} \frac{d}{dt}(r^2\dot{\theta})$$

which gives, by substitution in equation (11)

$$(15) \quad \frac{1}{r} \frac{d}{dt}(r^2\dot{\theta}) = \frac{Be}{m}\dot{r}$$

Integrating:

$$(16) \quad \int d(r^2\dot{\theta}) = \int \frac{Be}{m} r \dot{r} dt = \frac{Be}{m} \int_{r_0}^r r dr$$

$$r^2\dot{\theta} = \frac{Be}{m} \frac{(r^2 - r_0^2)}{2}$$

$$(17) \quad \dot{\theta} = \frac{Be}{2m} \left[1 - \left(\frac{r_0}{r} \right)^2 \right]$$

Assuming:

$$(18) \quad \dot{e}(r_c) = 0$$

r_c = cathode radius

Giving

$$(19) \quad \dot{e} = \frac{Be}{2m} \left[1 - \left(\frac{r_c}{r} \right)^2 \right]$$

Substituting equation (19) in equation (10) gives:

$$(20) \quad \ddot{r} - r \left(\frac{Be}{2m} \right)^2 \left[1 - \left(\frac{r_c}{r} \right)^2 \right]^2 + \frac{r}{2} \left(\frac{Be}{m} \right)^2 \left[1 - \left(\frac{r_c}{r} \right)^2 \right] + \frac{e}{m} E = 0$$

or

$$\ddot{r} + r \left(\frac{Be}{2m} \right)^2 \left\{ - \left[1 - \left(\frac{r_c}{r} \right)^2 \right]^2 + 2 - 2 \left(\frac{r_c}{r} \right)^2 \right\} + \frac{e}{m} E = 0$$

which becomes

$$\ddot{r} + r \left(\frac{Be}{2m} \right)^2 \left[-1 + 2 \left(\frac{r_c}{r} \right)^2 - \left(\frac{r_c}{r} \right)^4 + 2 - 2 \left(\frac{r_c}{r} \right)^2 \right] + \frac{e}{m} E = 0$$

giving the equation of radial motion:

$$(21) \quad \ddot{r} + r \left(\frac{Be}{2m} \right)^2 \left[1 - \left(\frac{r_c}{r} \right)^4 \right] + \frac{e}{m} E = 0$$

The solution of this equation using the values of E and B in the tube, where B is in the \hat{z} direction only and E consists of a radial term only, should give information as to the tube transit times.

For B assumed constant, and values of E found by differentiating the potential, found with the electrolytic tank or assumed from space charge considerations;

$$(22) \quad E = - \frac{dV}{dr} \hat{r}$$

V = potential at point R

Numerical calculations of electron paths have been made and are shown in Figures 21 and 22. The numerical calculations were made using the following difference equation obtained from Dr. Milne.

$$(23) \quad r_{(n+1)} = 2r_{(n)} - r_{(n-1)} + h^2 f(r)_{(n)}$$

for solving the differential equation;

$$(24) \quad \ddot{r} = f(r)$$

where

$$(25) \quad h = t_{(n)} - t_{(n-1)} = t_{(n+1)} - t_{(n)}$$

and the tabulation was as follows:

t in sec.	r in meters	$h^2 f(r)$ in meters
$t_{(n-1)}$	$r_{(n-1)}$	$h^2 f(r)_{(n-1)}$
$t_{(n)}$	$r_{(n)}$	$h^2 f(r)_{(n)}$
$t_{(n+1)}$	$r_{(n+1)}$	$h^2 f(r)_{(n+1)}$

There are more accurate numerical formulas than this but the work involved in using them is much greater. Considering the graphical method used for finding E in $f(r)$, and the smoothness of the functions involved, the results obtained by the above methods should be sufficiently

accurate. A rough estimate of the error indicates that it should be in the order of a few per cent at most.

The electric field E was calculated by measuring the slope of curves of potential versus radius which had been plotted from electrolytic tank data or space charge assumptions.

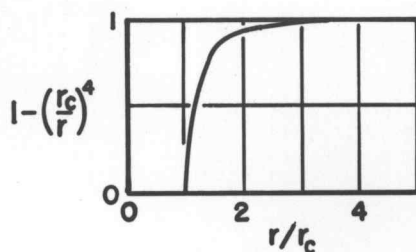
The equation

$$(26) \quad f(r) = -r \left(\frac{Be}{2m} \right)^2 \left[1 - \left(\frac{r_c}{r} \right)^4 \right] - \frac{e}{m} E$$

can be discussed further as follows: the term

$$(27) \quad 1 - \left(\frac{r_c}{r} \right)^4$$

is a function which approaches unity rapidly as r increases, especially if r_c is small.



The term

$$(28) \quad \frac{Be}{2m}$$

is known as the Lamar frequency of electron motion and indicates approximately the frequency of electron cyclic motion in co-axial structures with axial magnetic field and no space charge.

Consider

$$(29) \quad r \left(\frac{Be}{2m} \right)^2 \left[1 - \left(\frac{r_c}{r} \right)^4 \right] = \frac{e}{m} E^*$$

E^* = fictitious "magnetic" field

as defining E^* , giving

$$(30) \quad f(r) = - \frac{e}{m} (E + E^*)$$

Since

$$(31) \quad E = - \frac{dV}{dr}$$

It is assumed that

$$(32) \quad E^* = - \frac{dV^*}{dr}$$

V^* = fictitious "magnetic" potential

It should be pointed out that these fictitious fields and potentials represent values of electric field and potential which, when added to those already present would cause, with no magnetic field, the same radial behavior as that observed with the magnetic field. The e components of motion in the two cases would be quite different. The magnitude of the fictitious magnetic potentials are shown in Figures 21 and 22 for the conditions indicated.

From equation 32, assuming $V^*(r_c) = 0$,

$$(33) \quad V^* = - \int_{r_c}^r E^* \cdot dr$$

where

$$(34) \quad E^* = \left(\frac{Be}{2m}\right)^2 \left[1 - \left(\frac{r_c}{r}\right)^4 \right] r$$

then

$$(35) \quad \begin{aligned} V^* &= -\left(\frac{Be}{2m}\right)^2 \int_{r_c}^r \left(r - \frac{r_c^4}{r^3} \right) dr \\ &= -\left(\frac{Be}{2m}\right)^2 \left(\frac{r^2}{2} + \frac{1}{2} \frac{r_c^4}{r^2} \right) \Big|_{r_c}^r \\ &= -\frac{1}{2} \left(\frac{Be}{2m}\right)^2 \left(r^2 - r_c^2 + \frac{r_c^4}{r^2} - r_c^2 \right) \\ &= -\frac{r^2}{2} \left(\frac{Be}{2m}\right)^2 \left[1 - 2\left(\frac{r_c}{r}\right)^2 + \left(\frac{r_c}{r}\right)^4 \right] \\ (36) \quad V^* &= -\frac{r^2}{2} \left(\frac{Be}{2m}\right)^2 \left[1 - \left(\frac{r_c}{r}\right)^2 \right]^2 \end{aligned}$$

Cut-off value will occur where $V^* = -V$ in the tube. A nomogram of this condition is presented in Figure 24.

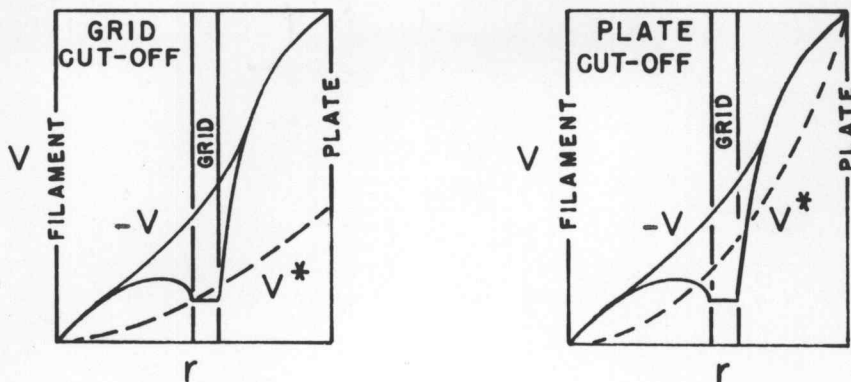


Figure 25. Grid and Plate Cut-off Conditions

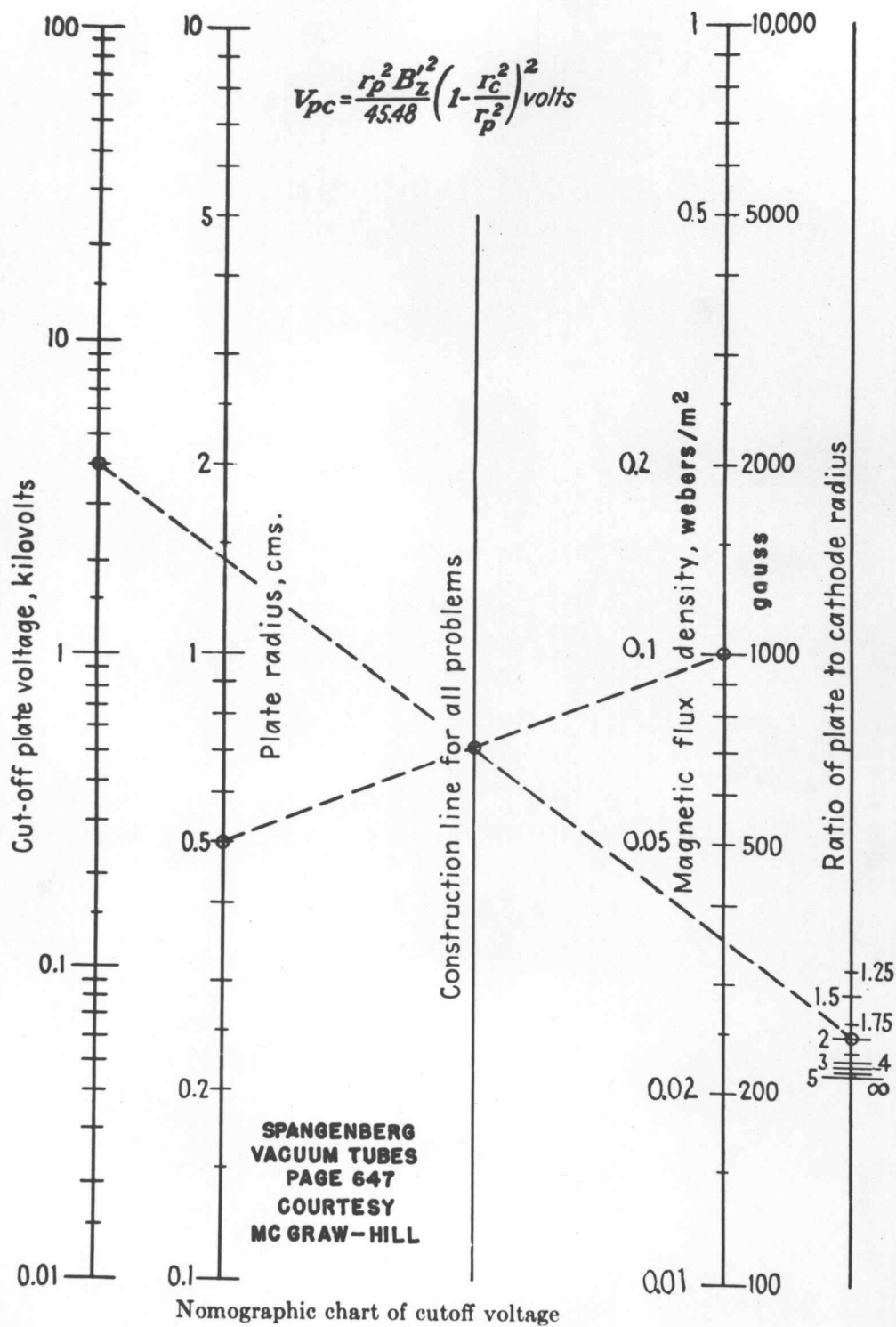


Figure 24

Where this happens the electrons will stop their outward travel and go back toward the cathode.

If space charge conditions are considered, a completely accurate analysis of the potential distribution within the tube would be exceedingly difficult. However, with the aid of some empirical relations for magnetrons and space charge limited triodes it was possible to assume potential distributions which seemed somewhat reasonable. The maximum potentials at the grid radius, for no magnetic field, were assumed to be the sum of the grid bias and the quotient of the plate voltage divided by the amplification factor (assumed to be 10). A linear distribution was assumed from the cathode to the grid and from the grid to the plate. For conditions of magnetic field and zero grid bias, a potential slightly greater than that necessary to produce cut-off was assumed to exist at the grid radius and the potential distributions from this point to the cathode and plate were assumed to be linear. With magnetic fields and grid biases of magnitudes approximating grid cut-off it was assumed that the potential in the grid region was equal to the grid bias and that a virtual cathode existed, having that radius which would provide cut-off for the conditions of grid voltage and magnetic field used. It was assumed that the entire cathode-plate potential drop was linear from this virtual cathode to the plate surface. With these assumptions the calculations resulting in the data

presented in Figure 22 were carried out.

APPENDIX II

TRANSIT TIME EFFECT ON GRID CONDUCTANCE

One of the first and most important effects of transit time is a large increase in grid power consumed. An investigation of the current induced in the grid leads by the electrons in transit from the cathode to the plate will help to explain this effect.

A plot of approximate electron velocities for a typical triode is shown in Figure 26.

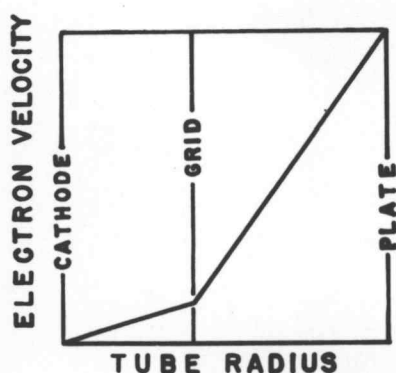


Figure 26. Electron Velocity

The electron transit time for such a tube is shown in Figure 27.

Combining this velocity distribution and transit time information the value of induced grid current can be found.

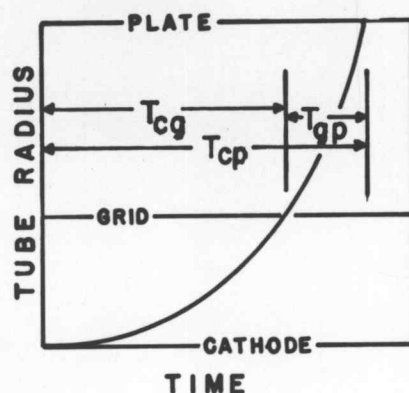


Figure 27. Transit Time

Investigating the current induced by an electron leaving the grid at the instant of the positive peak of grid voltage it is found, Figure 28, that first a positive current is induced as the electron approaches the grid, then a negative one as it goes away.

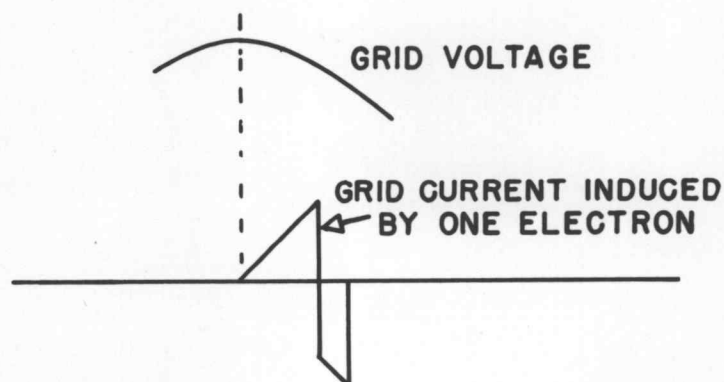


Figure 28. Induced Grid Current

The positive and negative induced grid current contributions are considered separately thus giving two a-c

components with the same frequency as the oscillation and two equal and opposite d-c components.

The grid voltage and current from the external resonant circuit are in phase quadrature as shown in Figure 29.

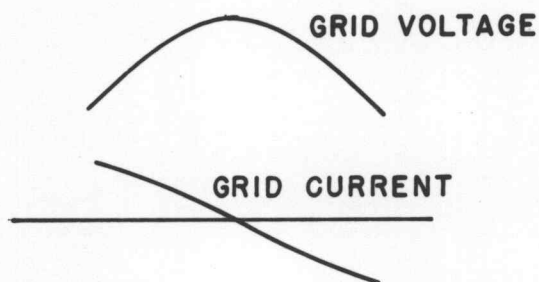


Figure 29. Applied Grid Current

Transit angles, ϕ and θ are defined as the transit time, T , measured in terms of the phase angle at some particular frequency, f . Thus,

$$\theta = 2\pi f T_{cg}$$

$$\phi = 2\pi f T_{cp}$$

where T_{cg} , is the cathode-grid transit time and T_{cp} , is the cathode-plate transit time.

The electron current leaving the cathode is essentially in phase with the grid voltage so that the positive component of grid current will lag the grid voltage by an angle, α , where $0 < |\alpha| < |\theta|$. The negative component will lag by an angle, β , where $|\theta| < |\beta| < |\phi|$.

A vector diagram of the resulting grid voltage and

currents, Figure 30, indicates the source of the resultant grid current, one component of which is in phase with the grid voltage thus producing a power loss.

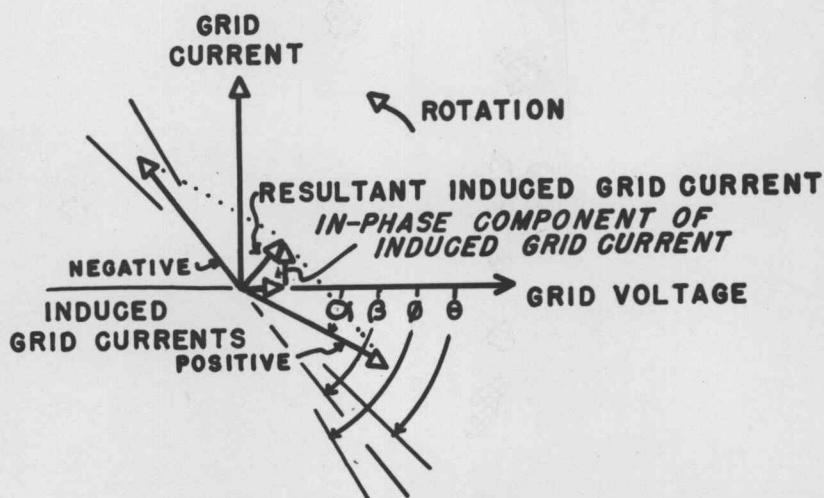


Figure 30. Vector Diagram

It can be seen that an increase in transit angle, either cathode-grid or grid-plate, would result in an increase in the magnitude of the resultant induced grid current, and bring it more nearly in phase with the grid voltage. Thus to a first approximation the grid conductance, that is the quotient of the in-phase component of the resultant induced grid current by the grid voltage, is proportional to the square of the transit angle, or the plate resistance, R , is inversely proportional to the square of the product of frequency and transit time

$$R = \frac{k}{f^2 T^2}$$

Usually a cathode-plate transit angle of π radians is considered to be the maximum for which oscillations are possible. Thus any reduction in either cathode-grid or grid-plate transit time will permit oscillation at a higher frequency because of the decreased grid losses.